



Deutsche  
Gesellschaft  
für Nuklearmedizin  
e.V.

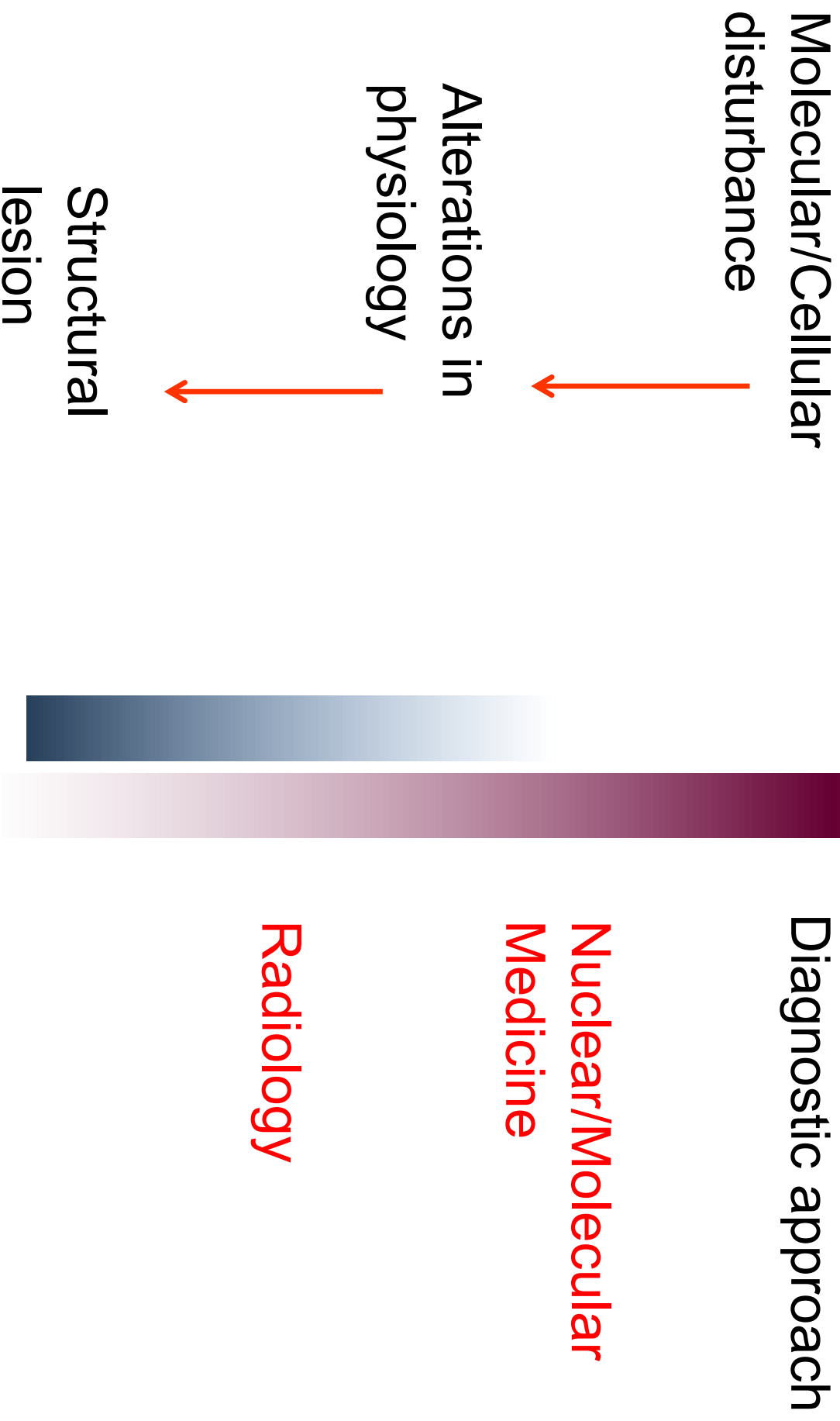
# Translational Research in Molecular Imaging and Radionuclid Therapy

August 31 – September 2, 2017

Overview Molecular Imaging  
PET and SPECT

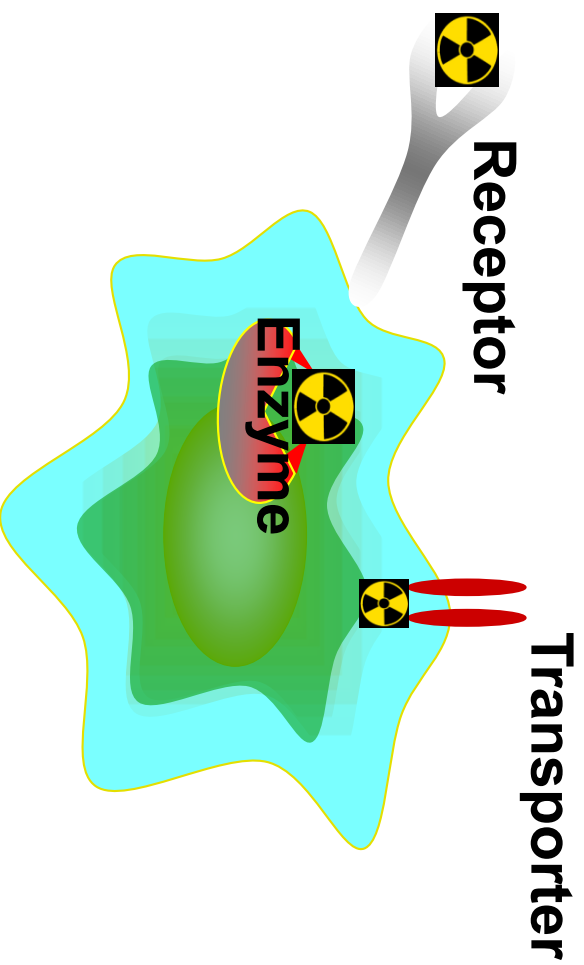
**UNIKLINIK**  
**RWTHAACHEN**  
KLINIK FÜR NUKLEARMEDIZIN  
F.M. Mottaghy

## Medical imaging and the pathology cascade



## Molecular interactions of radiolabeled probes

In vivo imaging of biological processes with radiolabeled molecular probes



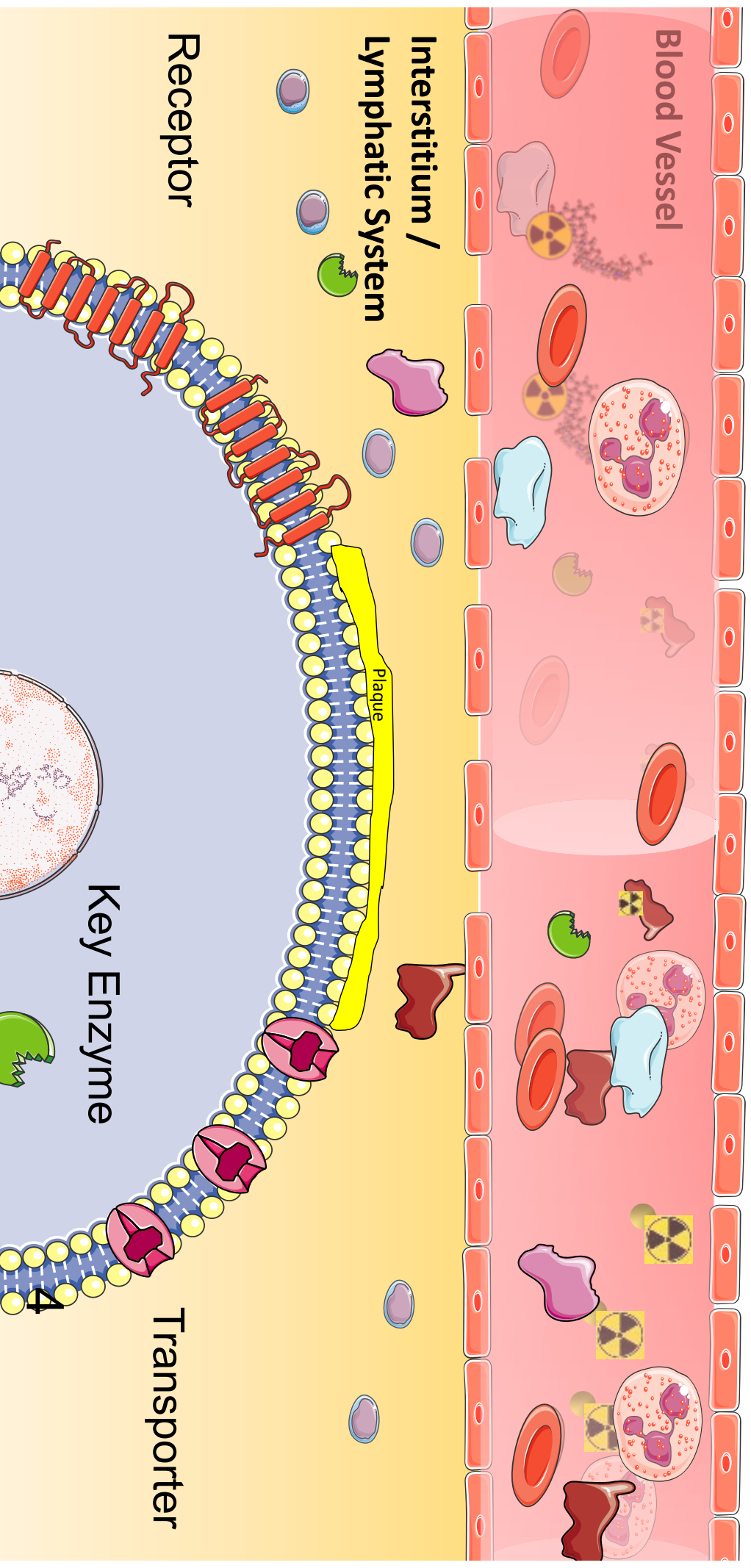
## Mechanism of localization

**Visualization of overexpression or increased activity of:**

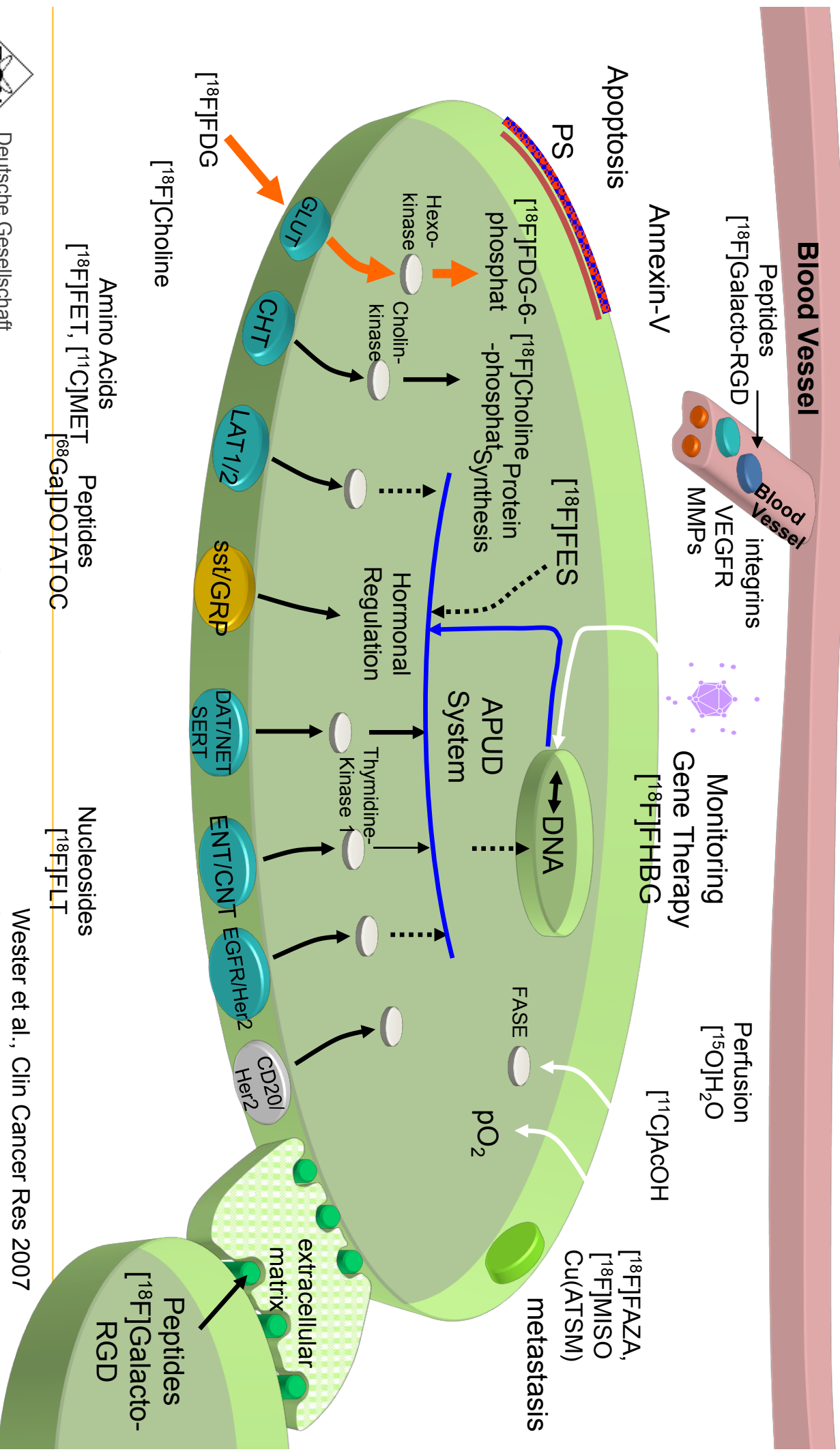
- Receptors
- Enzymes
- Transporters

# Nuclear Molecular Imaging

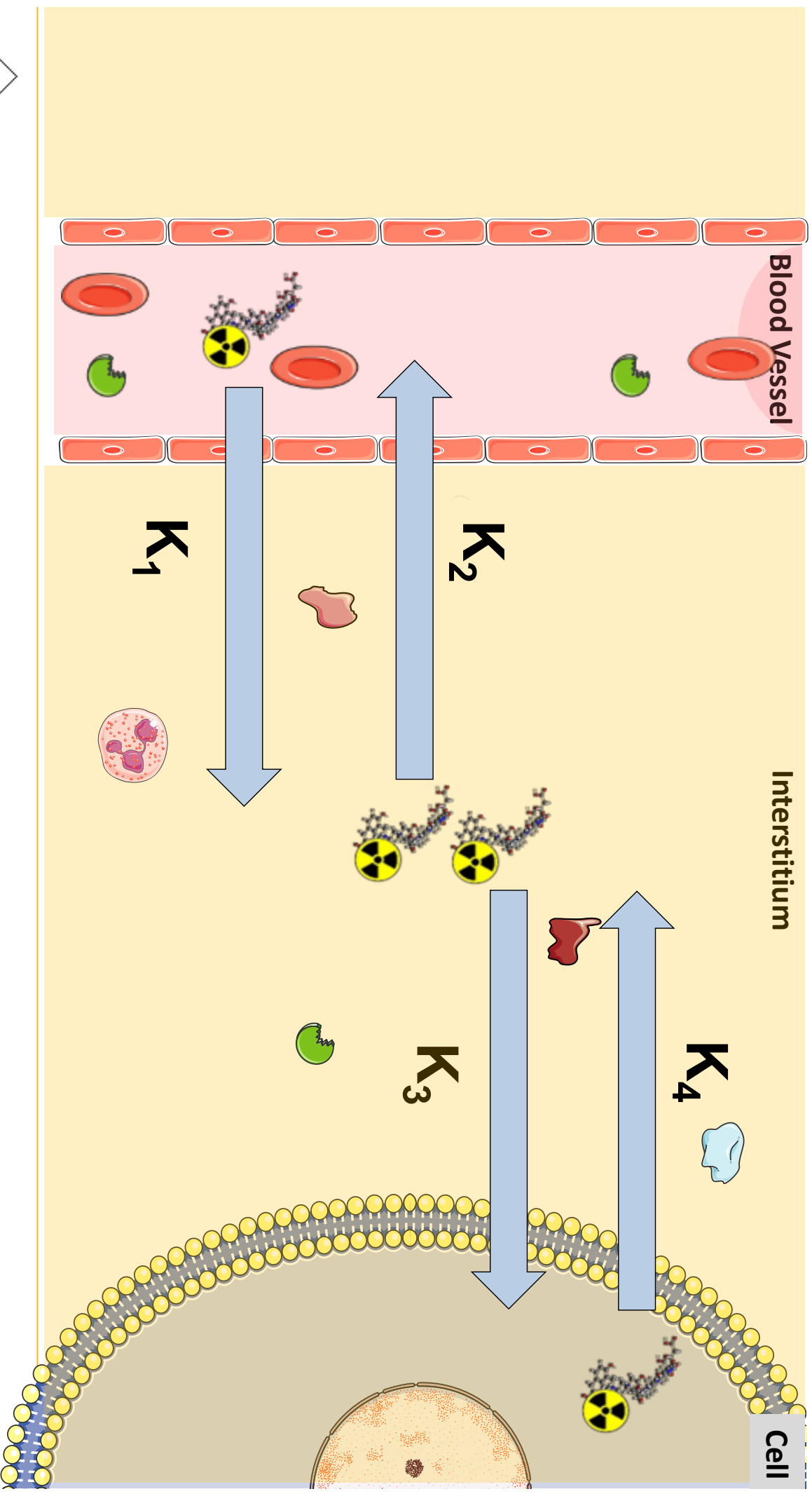
In vivo imaging of biological processes with  
radiolabeled molecular probes



# Molecular Probes (Tracers)



# COMPARTMENT MODEL





# Steps to molecular image acquisition

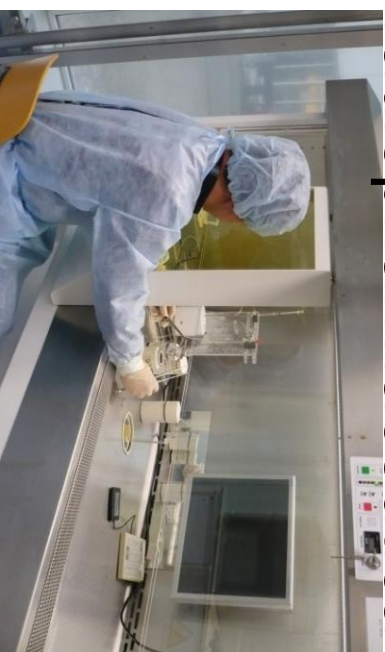
1.

Radionuclide



2. Synthesis of

radiopharmaceutical



3.

Radiopharmaceutical



4.

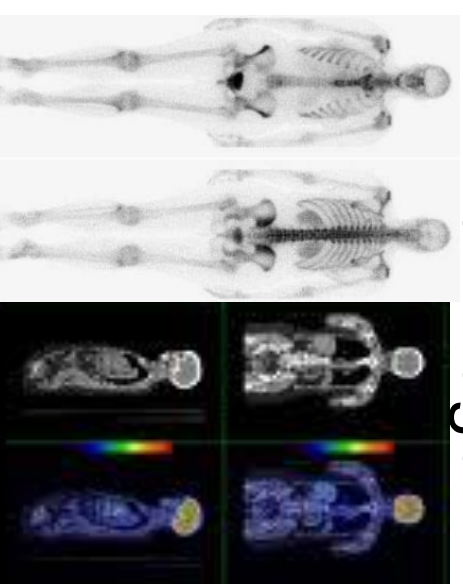
Application



5. Scan



6. Image



# Planar Scintigraphy

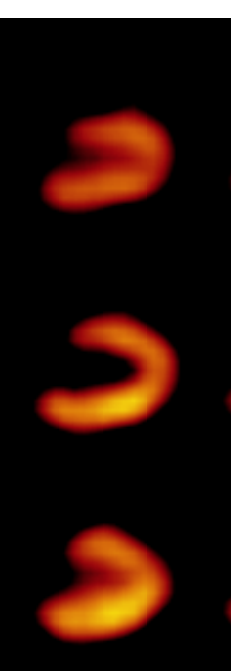
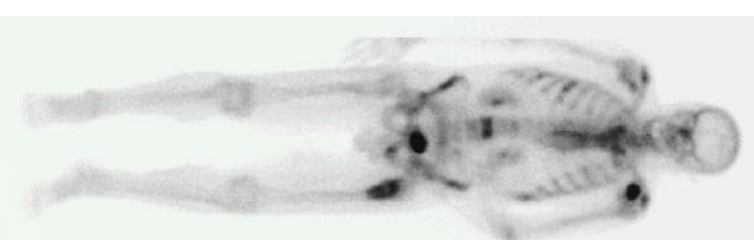
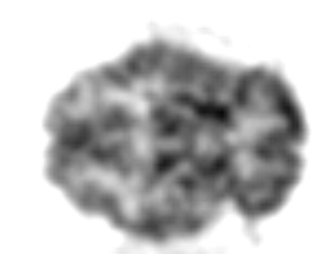
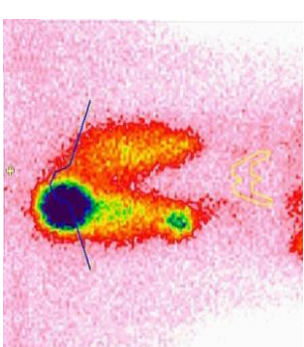
99mTc

6h HWZ  
140 keV

Nuklid

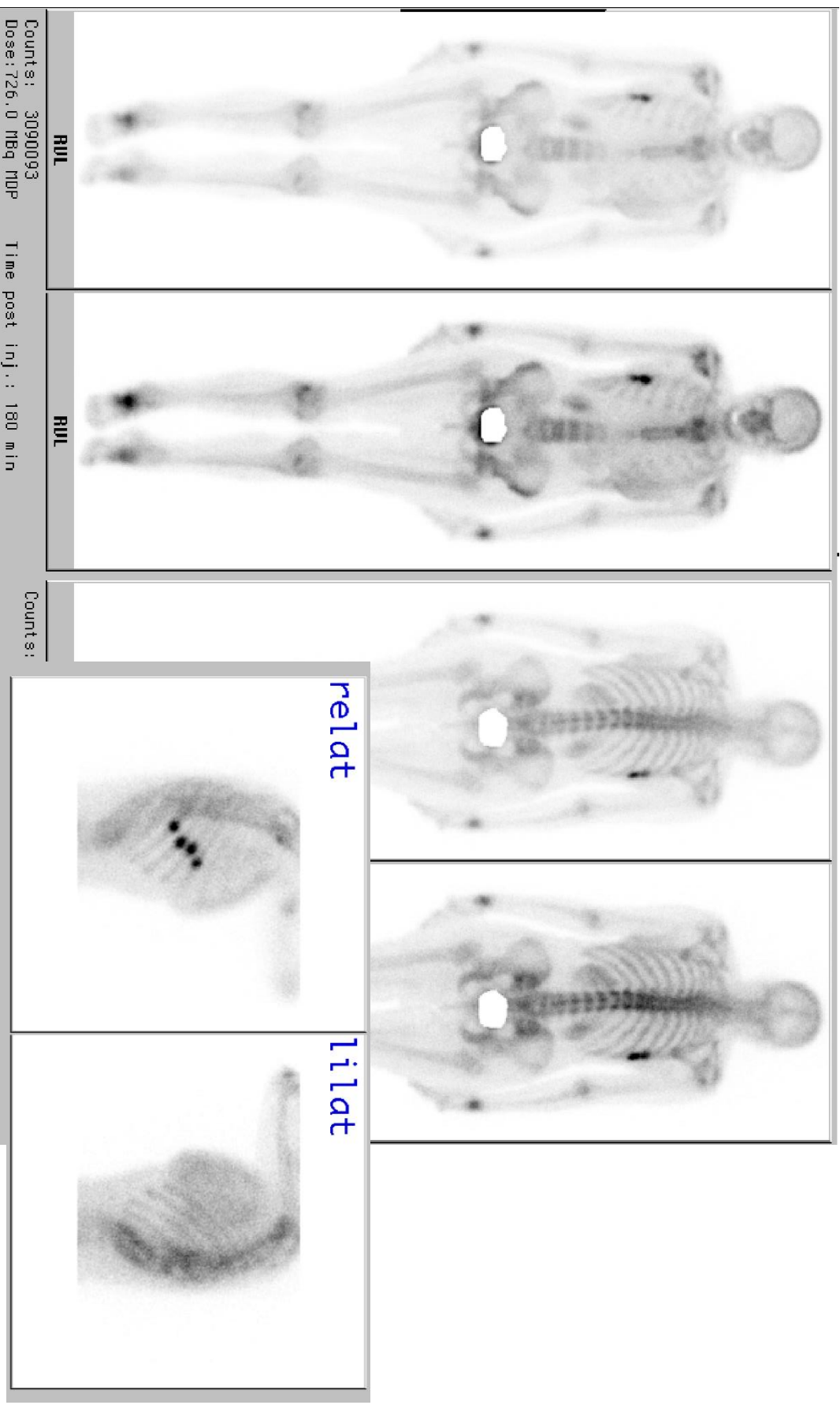


target-specific  
radiopharmaceuticals

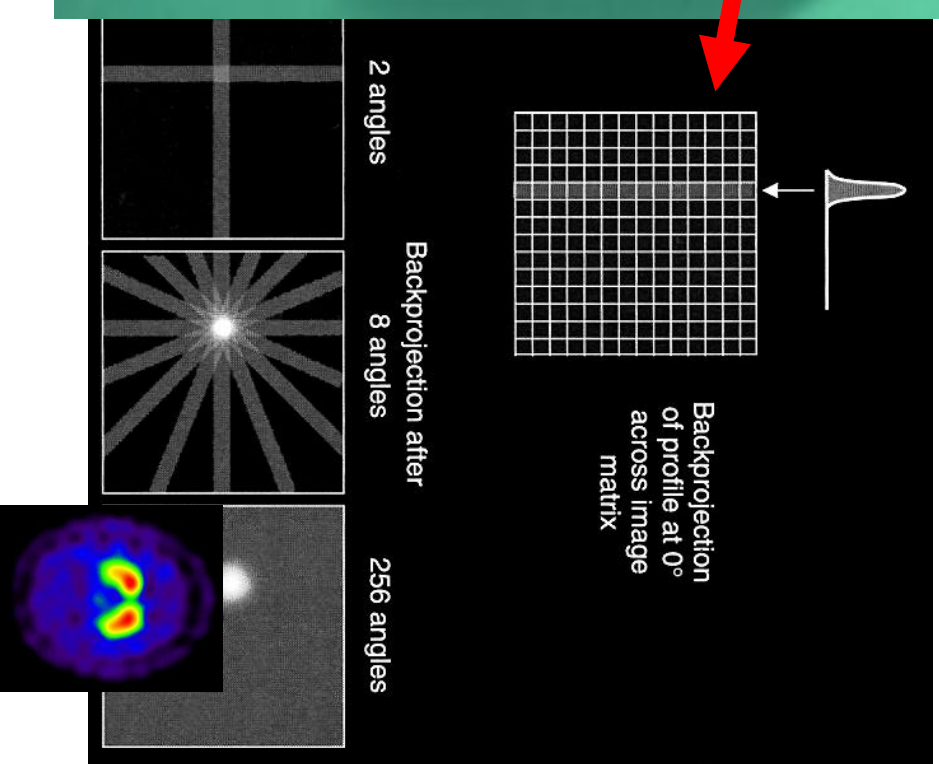
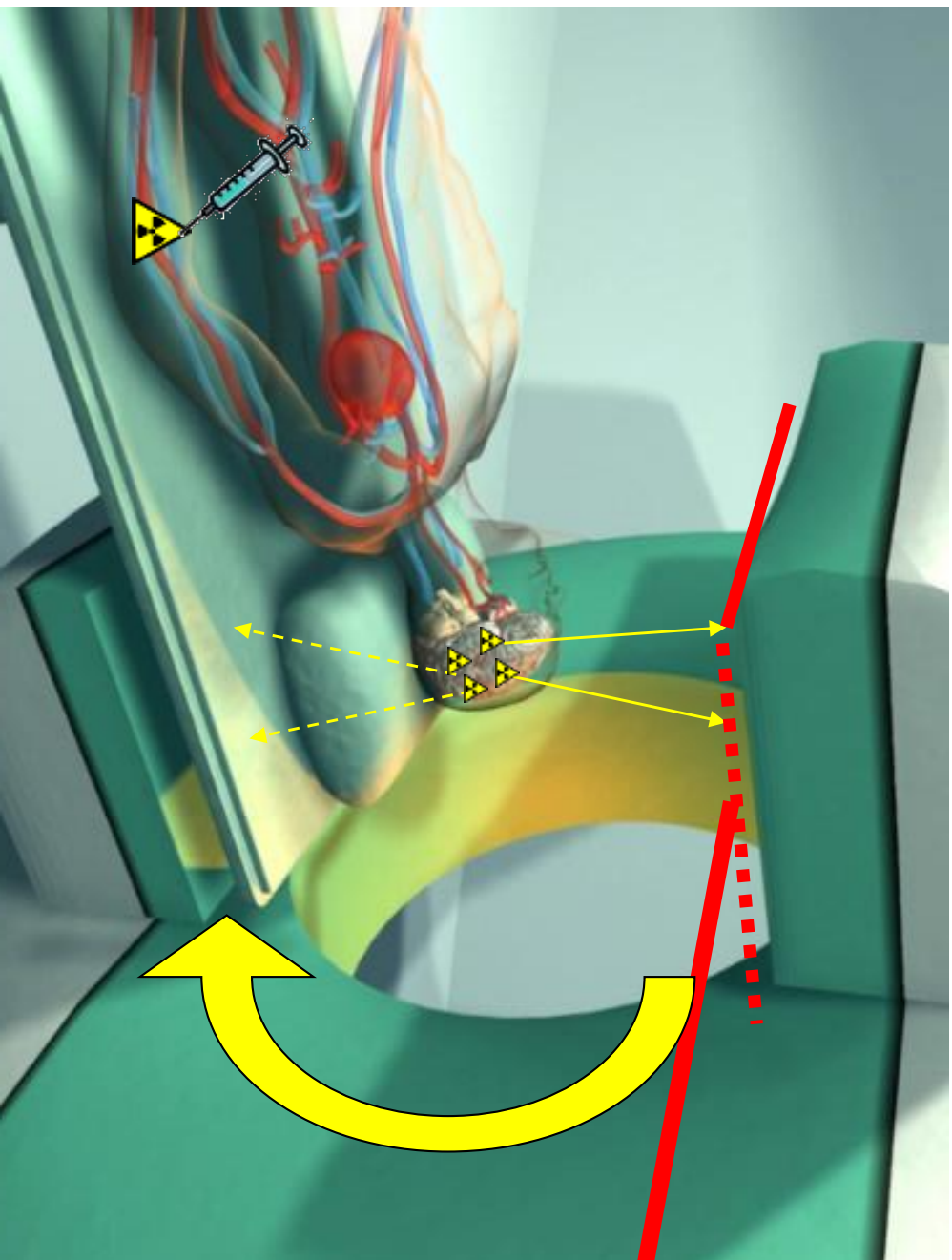




# Bone-Scintigraphy ( $^{99m}\text{Tc-MDP}$ )

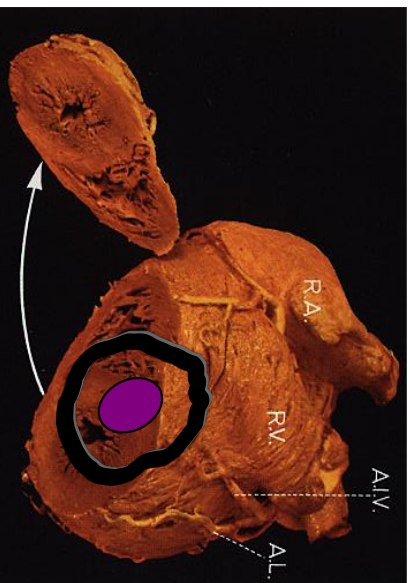


# Single Photon Emission Computed Tomography (SPECT)

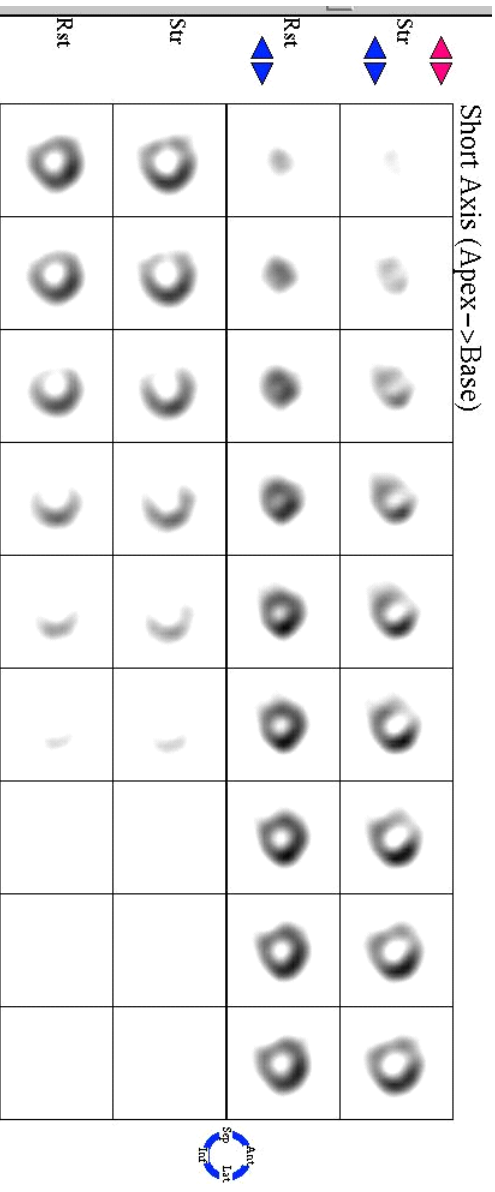


# Cardiovascular disease, ergometry until 75 Watt

## Myocardial SPECT



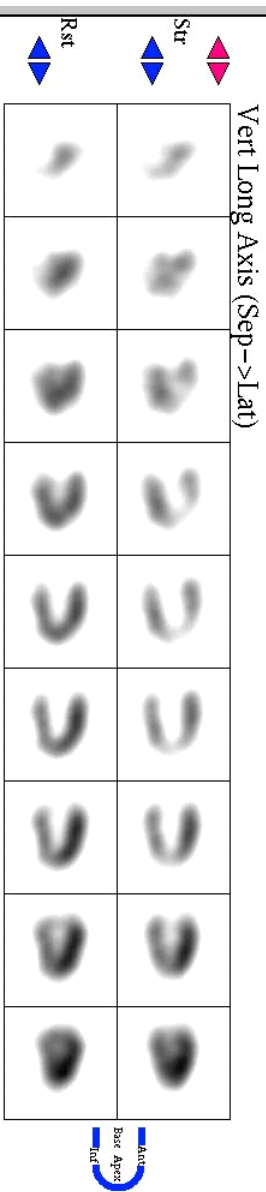
**short axis**



**horiz. long axis**

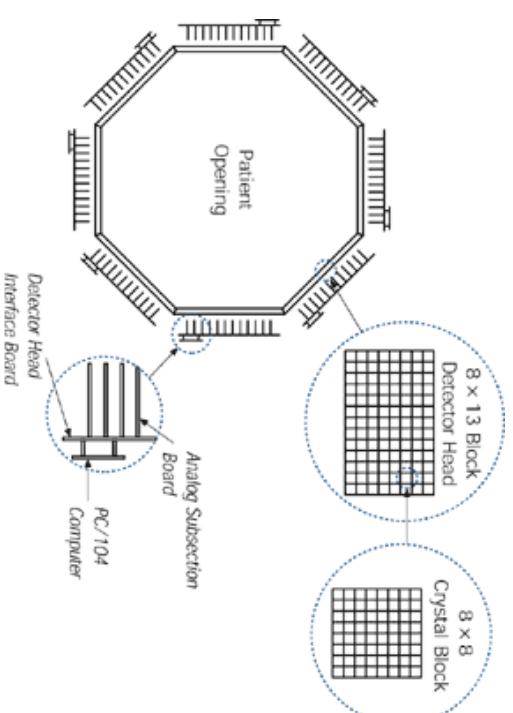
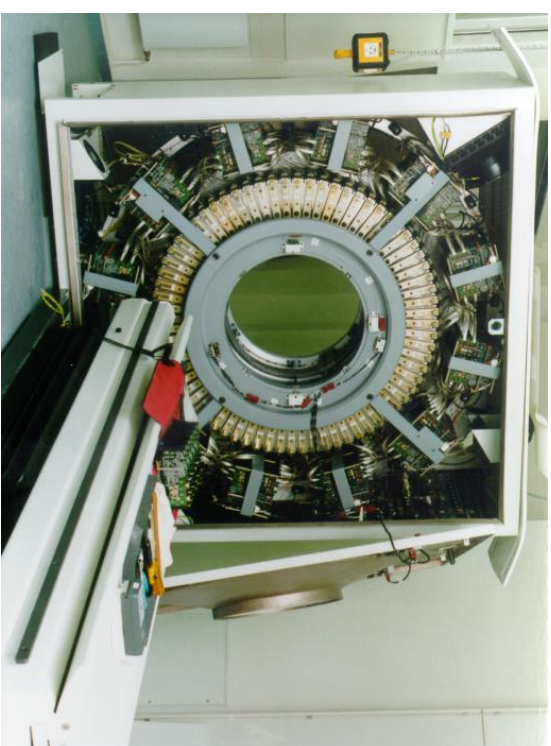


**vert. long axis**

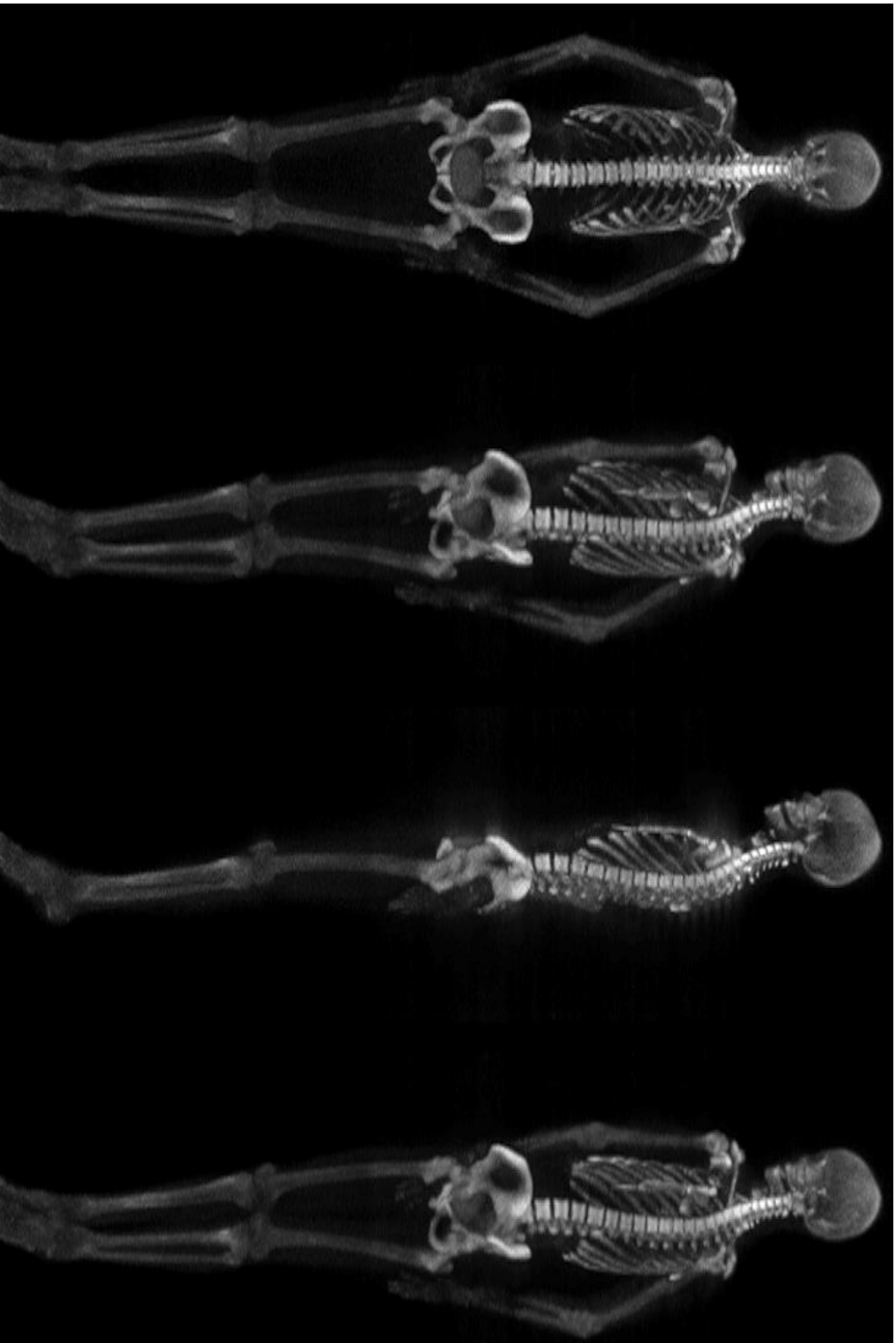




# Positronen-Emissions-Tomographie (PET)

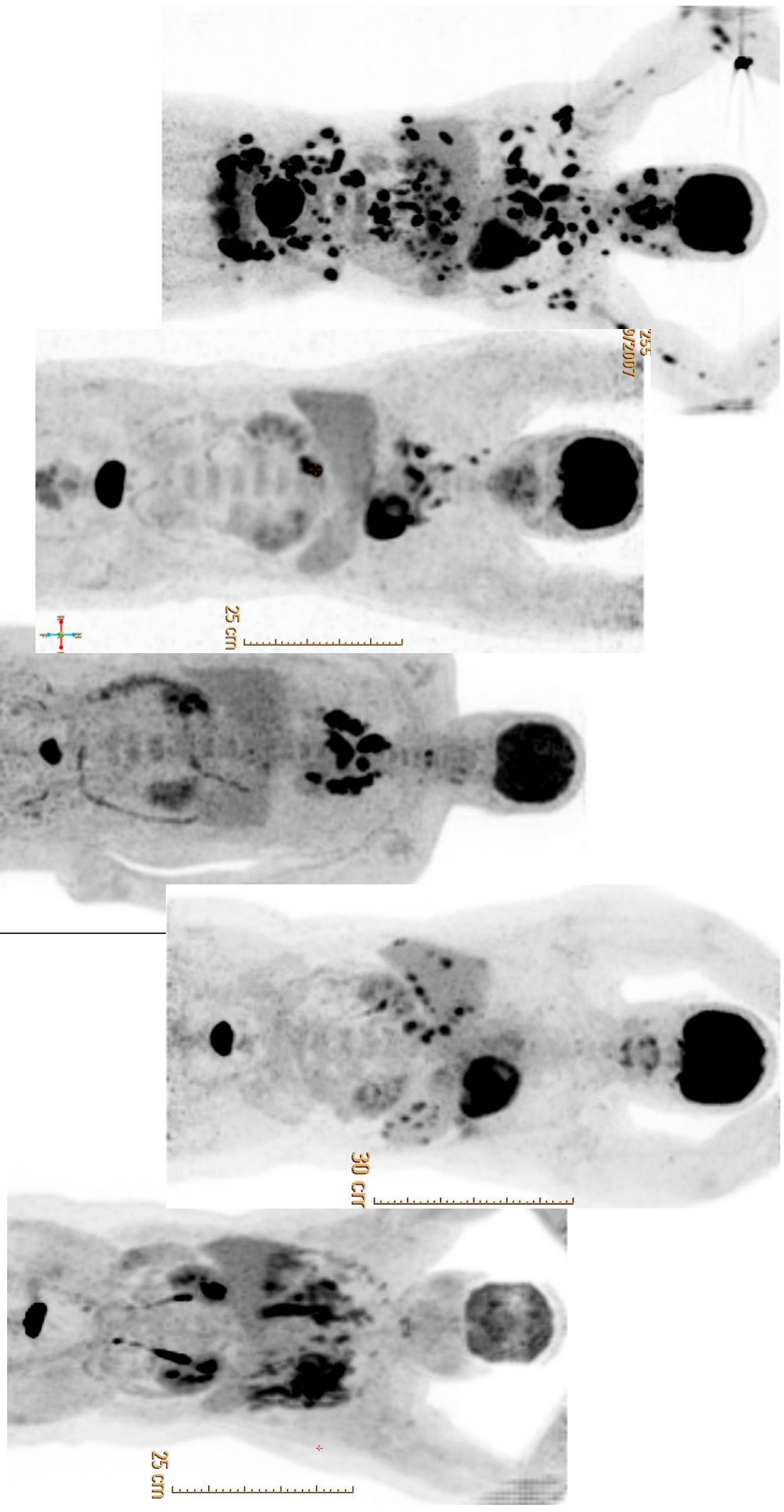


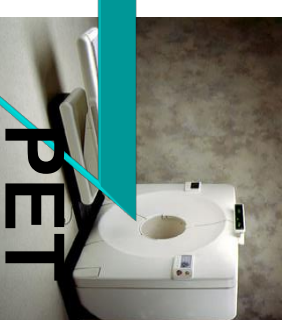
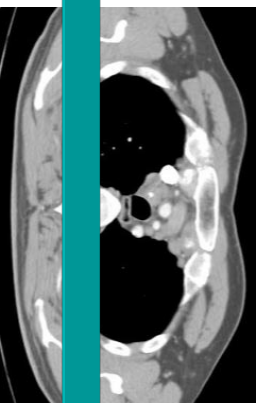
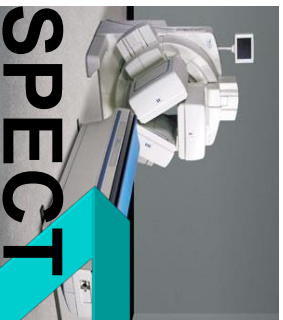
## **$^{18}\text{F}$ -Fluoride PET**



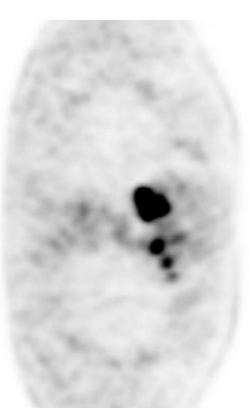
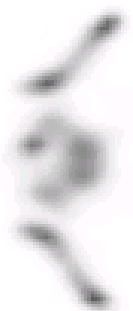
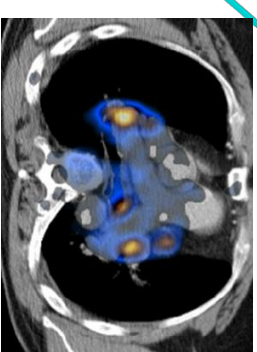


# Fluorodeoxyglucose-PET (Sarkoidosis)

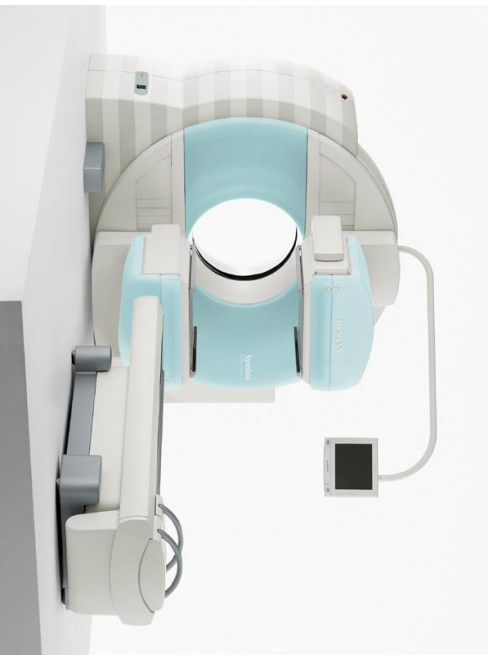




**Multimodal  
molecular/functional  
Imaging**



# SPECT/CT

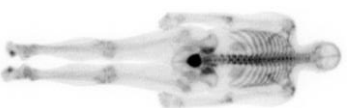


# SPECT/CT Prostate Cancer Bone Scan

## Staging I



L1



- Age 68 yrs., Post OP
- PSA increased
- Bone Scan,
- (745 MBq Tc-99m-HDP)
- SPECT/CT

## Staging II

### Pedicle of vertebral arch



L4



Posterior



L4



L4

## Staging III

### Metastasis Os sacrum



L4



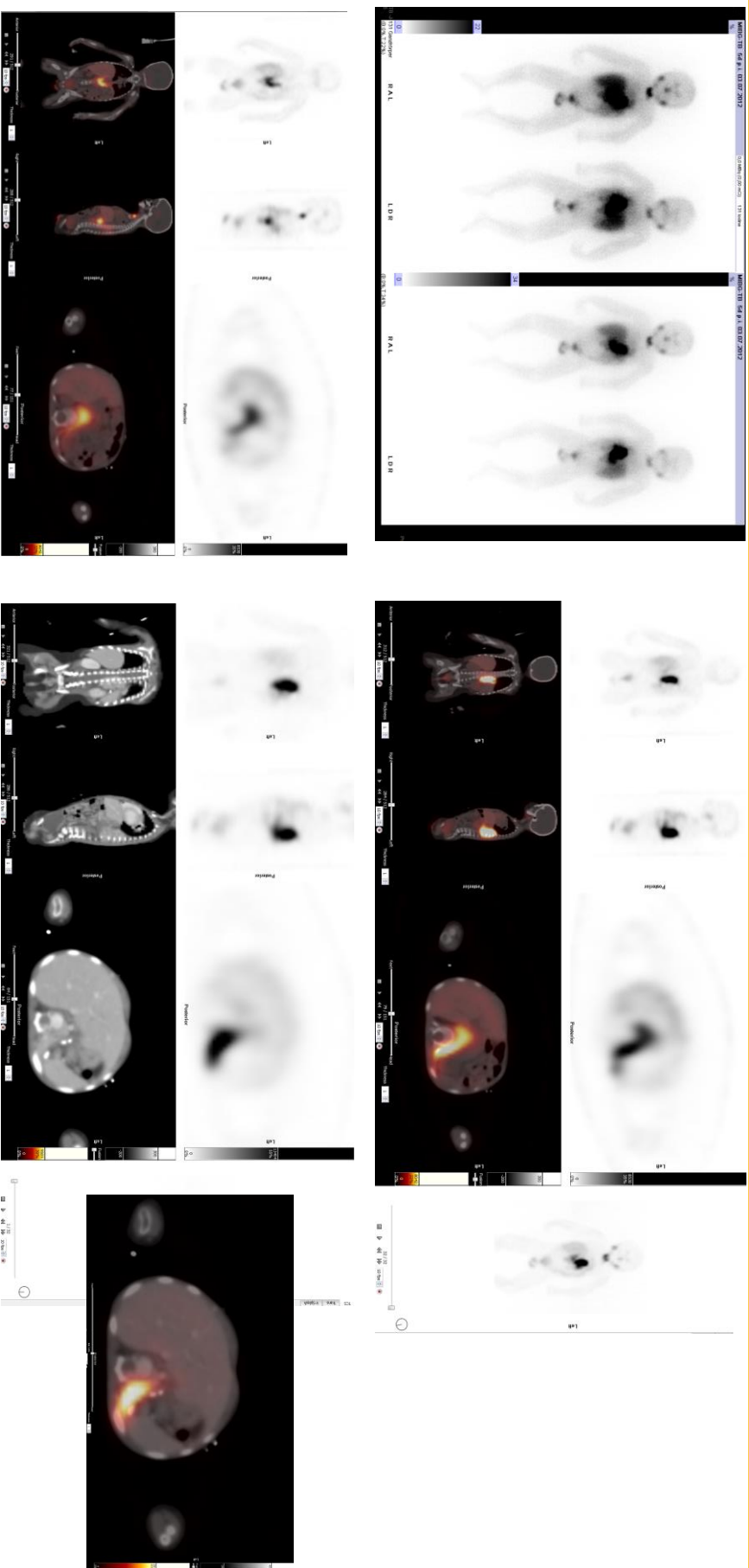
Posterior



L4



# MIBG SPECT/CT



- 2 yrs., Neuroblastoma Stage IV, post therapy, Neuroblastoma recurrence with cerebral and abdominal metastases, Tumour progress under recurrence therapy
- Planar imaging and SPECT/CT with contrast agent 5 days post therapy



# PET/CT





**Patient 1**

CRu (SPD – 84%)



**Patient 2**

PR (SPD – 55%)

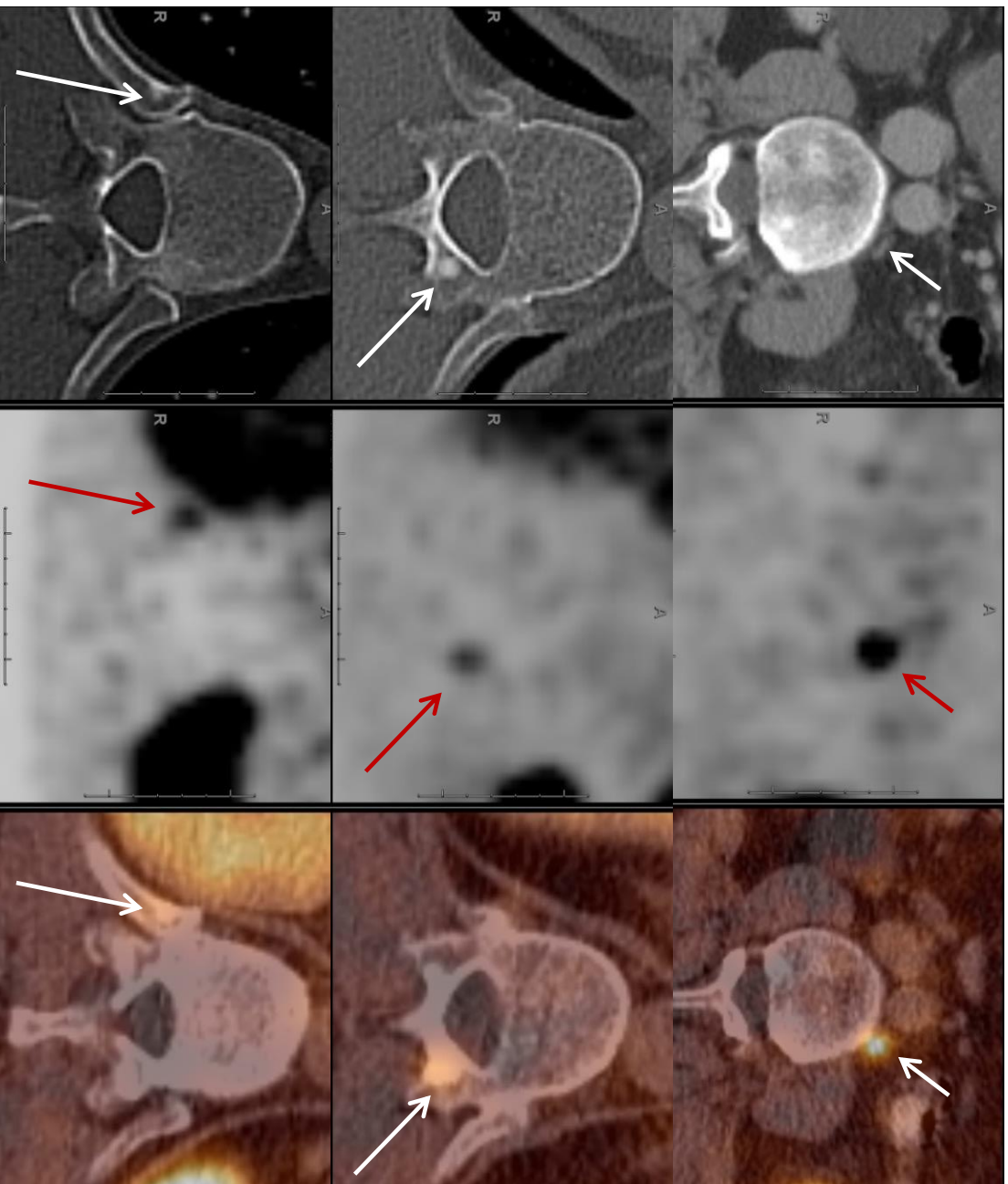


# PSMA PET/CT

CT

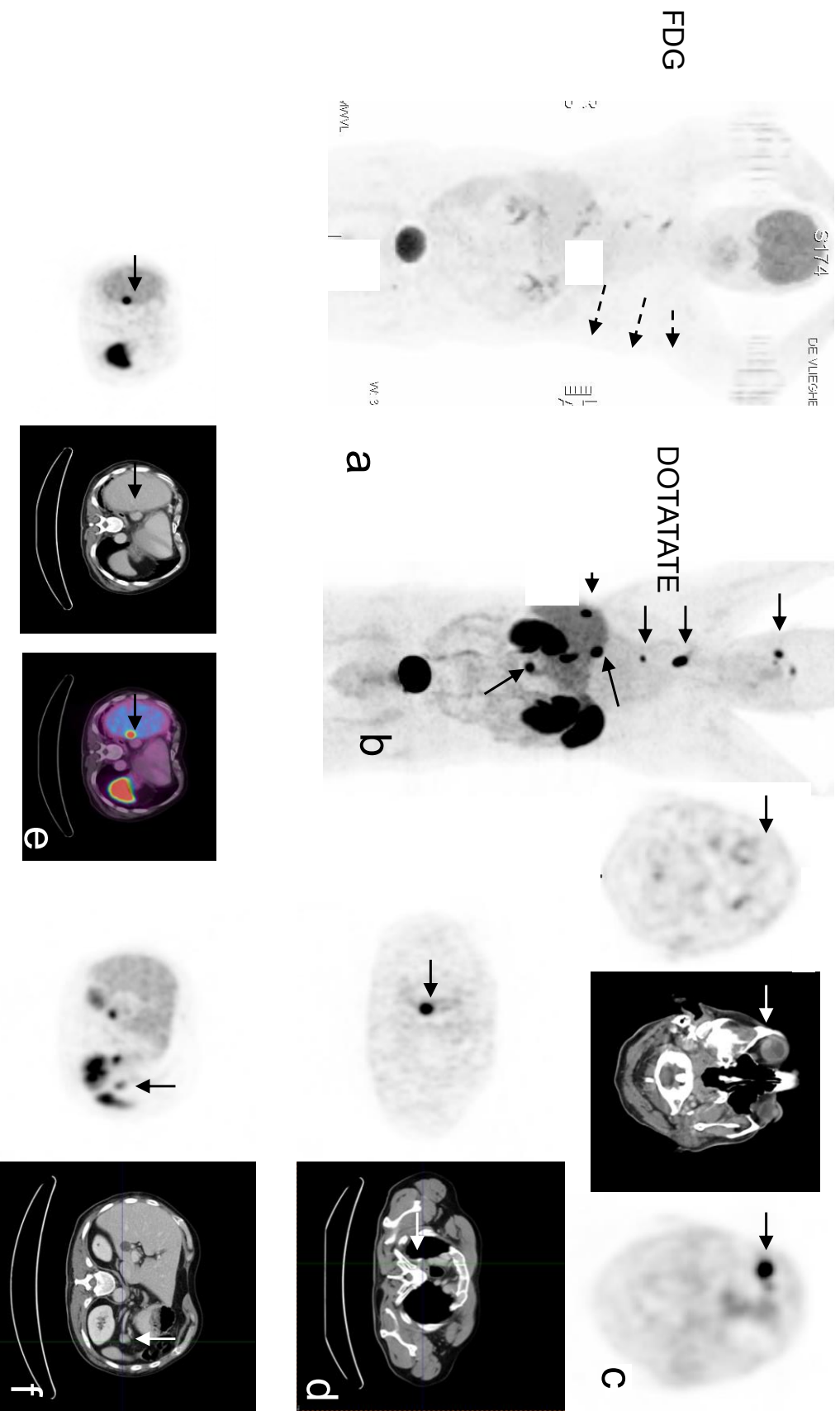
PET

Fusion





# Bronchial carcinoid with sudden onset of blurry vision

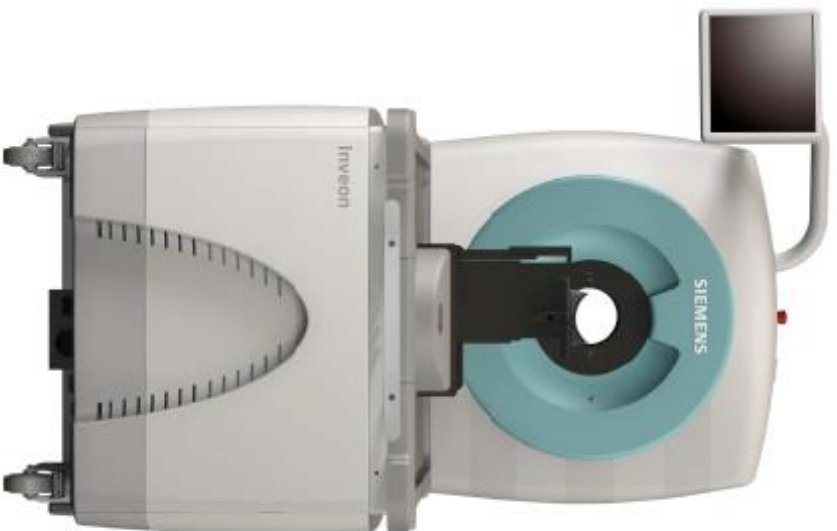


## Small animal imaging

- Important for development of new tracer
- Final preclinical step in the process from bench to bedside
- $\mu$ SPECT / CT
- $\mu$ PET / CT



## Small Animal Imaging / Model Examples



Small Animal -  
PET/CT



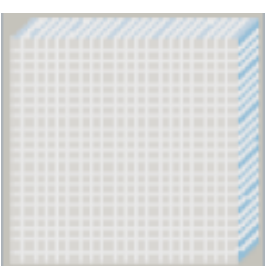
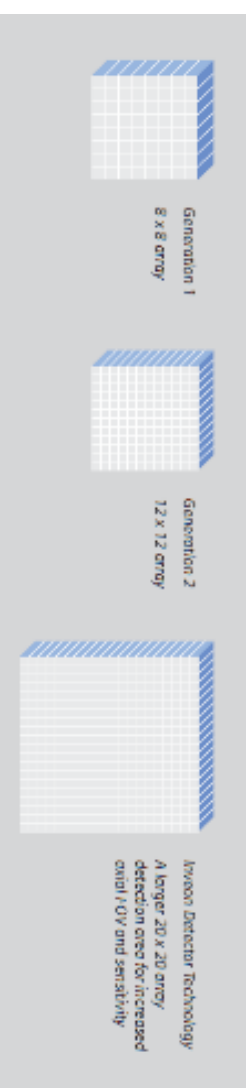
Small Animal  
SPECT/CT



Small Anir  
PET/SPEC

# Micro PET: Dedicated Small Animal System

Micro PET Siemens Inveon



Detector diameter:

16,1 cm

Transaxial FOV:

10,0 cm

Axial FOV:

12,7 cm

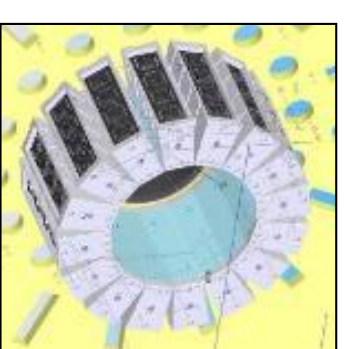
Crystal-detectors:

LSO - 64 Blocks

25600 Sum of single  
crystals



20x20 array



16 module

High resolution: 1,4 mm FWHM

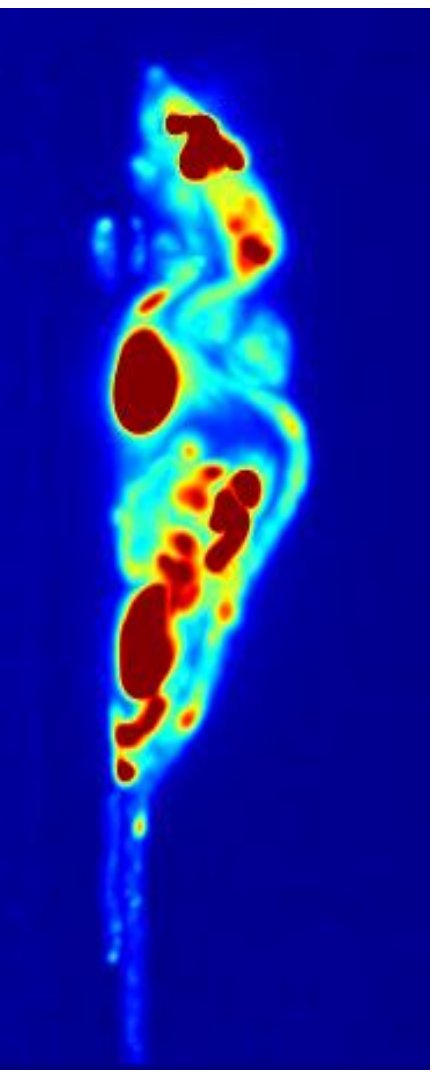
Absolut Sensitivity: 100,0 cps / 1KBq , 10 %

Micro PET - measurement of the glucose metabolism with  $^{18}\text{F}$ -FDG and of the skeleton with the bone affine radiopharmaceutical  $^{18}\text{F}$ -NaF in a mouse.

## $^{18}\text{F}$ -Sodium fluoride



## $^{18}\text{F}$ -Fluorodesoxyglucose



# Digital PET Sub-System



- Digital PET = direct coupling of scintillator to solid-state detectors
- No light sharing between detectors (better image quality)
- Patented Fast 3D Tomographic Image Reconstruction (December 2013)
- => Improved detectability of small lesions
- => High count rate capability from very low activity to 80MBq
- => Superior image quality with excellent contrast ratio

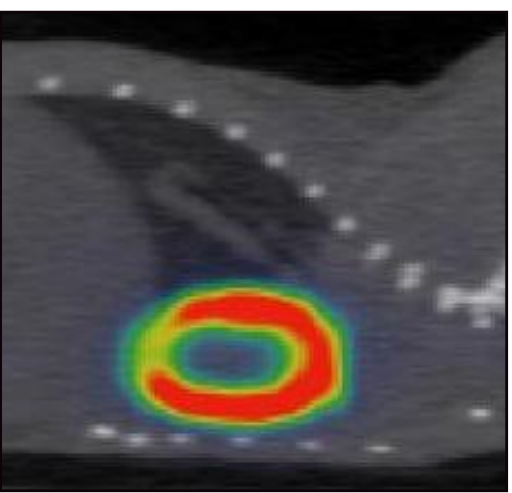
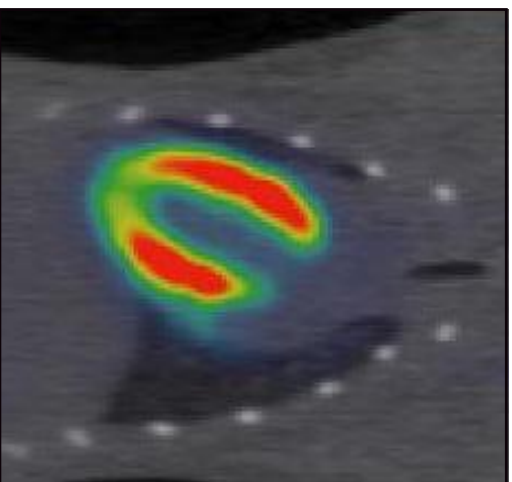
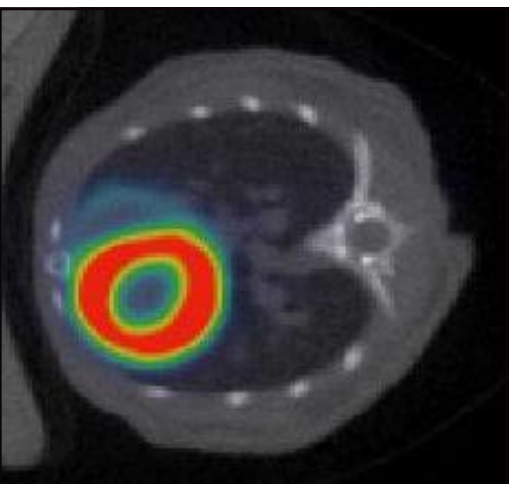
- ◆ Bore diameter: 15cm
- ◆ Transaxial FOV: User-selectable 46-100 mm
- ◆ Axial FOV: 30cm ( continuous motion)
  - LabPET4
  - LabPET8
  - LabPET12
- Quad-APD detector modules coupled with LYSO/LGSO phaswich scintillators
- Individual readout, parallel signal processing
- Fully integrated with SPECT and CT;
- field- upgradable

TriFoil

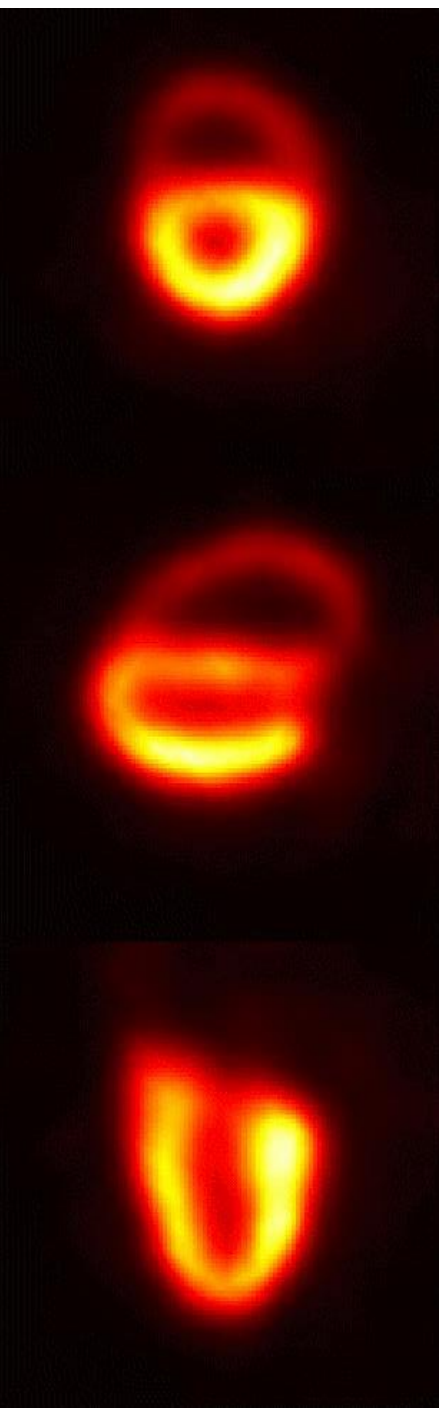


## PET/CT Cardiac Imaging - Mouse

PET/CT:  
0.7mCi of  
FDG, 20min.  
Post injection,  
5 min. scan



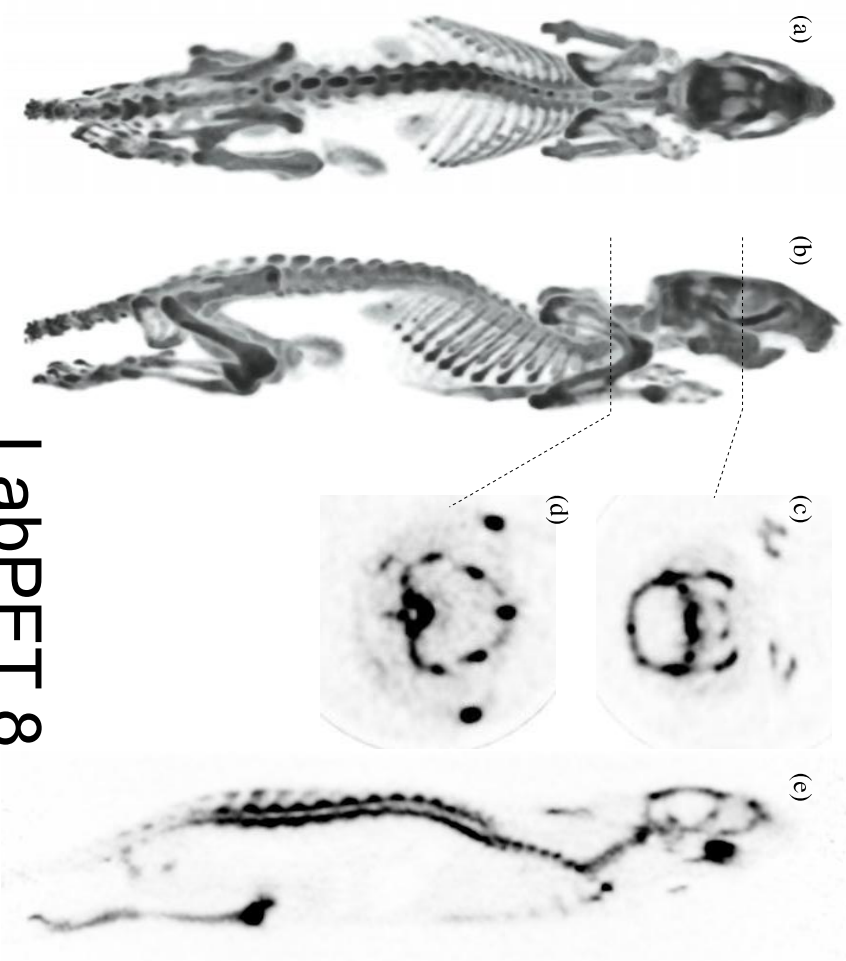
Detail of gated  
cardiac images



Courtesy of Dr. Ren-Shyan Liu, National Yangming University, Taipei, Taiwan

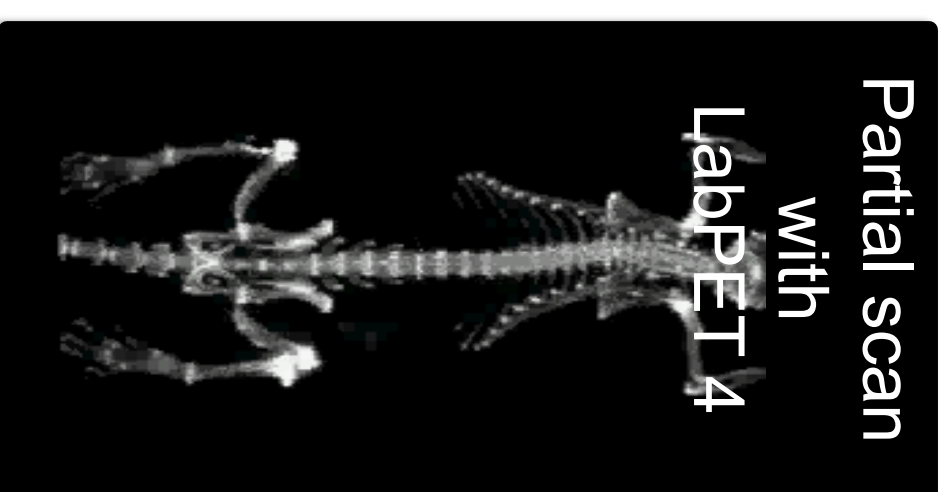


## Excellent isotropical resolution: 185 g rat



### LabPET 8

**Figure 10.** Volume-rendered images (a), (b) of a 185 g rat injected with 31 MBq of  $\text{Na}^{18}\text{F}$  and scanned 68 min post-injection on the LabPET8. Transaxial slices of the skull (c) and the ribcage (d) and a sagittal slice (e) are shown. The whole-body image was obtained by acquiring five overlapping decay-compensated scans with 3.78 cm steps for a total of 60 min. The image was obtained with a lower energy threshold of 350 keV and reconstructed using 80 3D MLEM iterations.



### TriFOIL

**Reference:** Imaging performance of LabPET APD-based digital PET scanners for pre-clinical research; M. Bergeron et al.; Université de Sherbrooke, QC, Canada; Phys. Med. Biol. 59 (2014) 1–18

## Small Animal Imaging / Model Examples



Small Animal -SPECT/CT

Small Animal -SPECT/CT

# MMP - S P E C T

Micro SPECT: Measurement of the bone skeleton with  $^{99m}\text{Tc}$ -HDP

Rat collimator

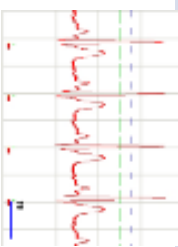
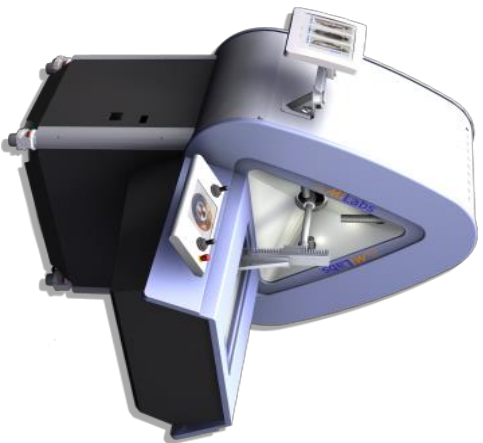


Rat -  $^{99m}\text{Tc}$ -HDP

Mouse collimator

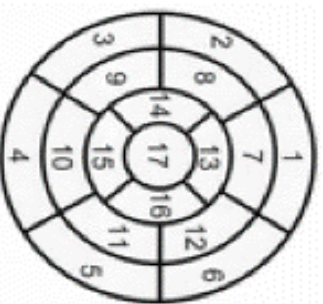
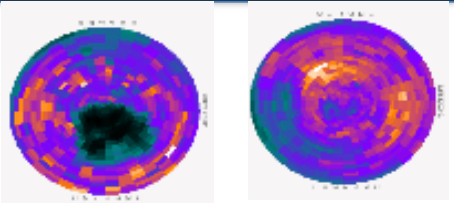
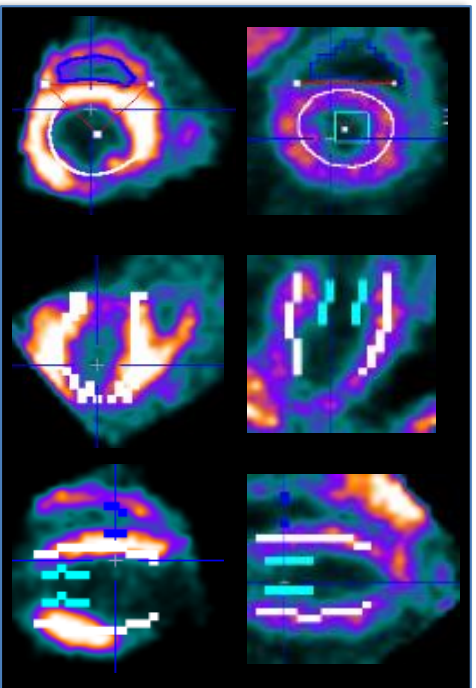


Mouse -  $^{99m}\text{Tc}$ -HDP

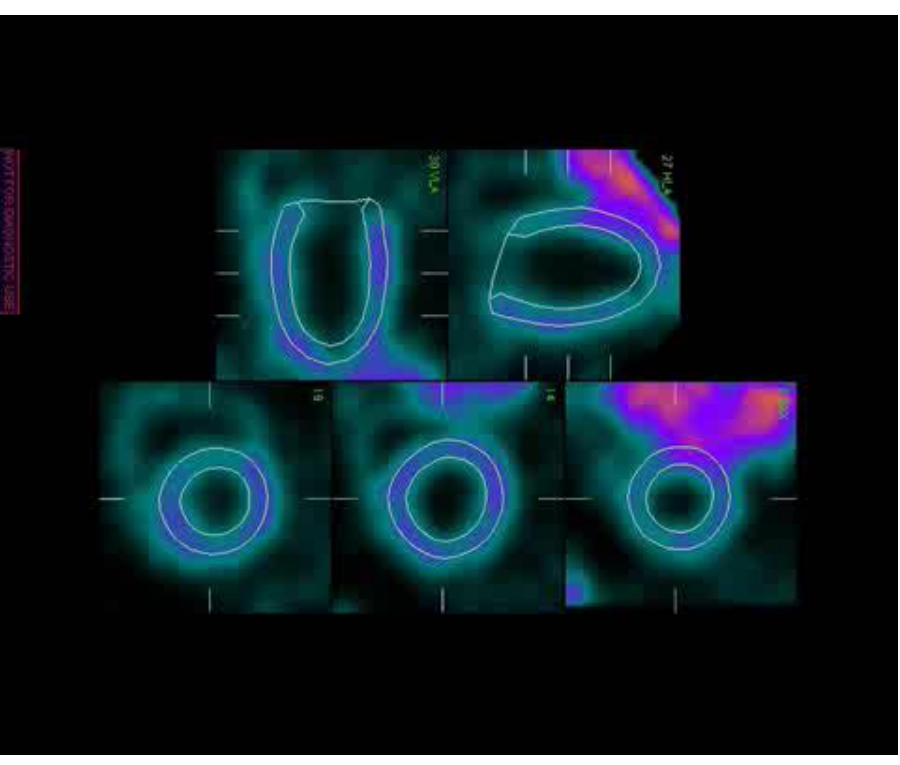


## ECG gating

## CARDIAC PMOD – 17 segment model



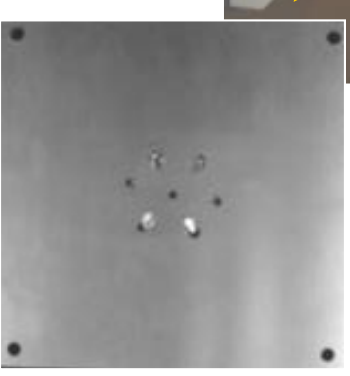
- 1. basal anterior
- 2. basal anteroseptal
- 3. basal inferoseptal
- 4. basal inferior
- 5. basal inferolateral
- 6. basal anterolateral
- 7. mid-anterior
- 8. mid-anteroseptal
- 9. mid-inferoseptal
- 10. mid-inferior
- 11. mid-inferolateral
- 12. mid-arterolateral
- 13. apical anterior
- 14. apical septal
- 15. apical inferior
- 16. lateral
- 17. apex





# Multiplex Multi Pinhole (MMP) - SPECT

- Micro SPECT: MMP-Technology with a clinically used SPECT gamma camera
- Physical measuring principals
- Characterisation and performance parameters



Siemens SPECT E.cam gamma camera

7-Pinhole Aperture Plate

# MMP - S P E C T

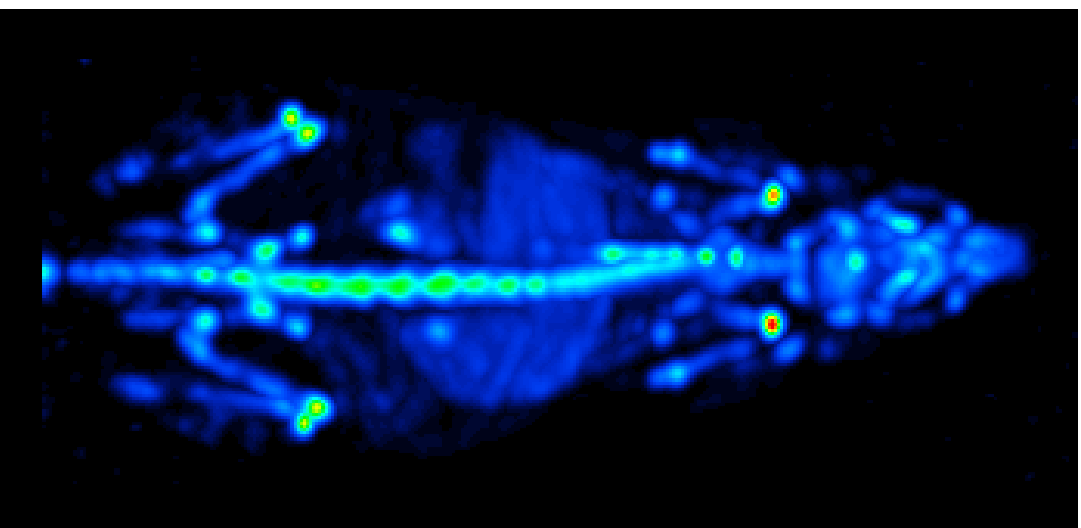


# MMP - S P E C T

Micro SPECT: Measurement with MMP-Technology by a clinically used SPECT gamma camera

## SPECT

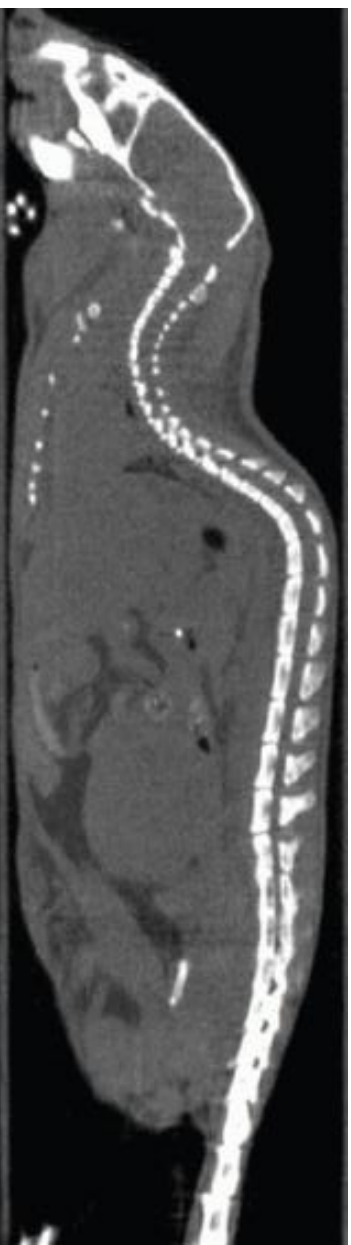
$^{99m}\text{Tc}$ -HDP



# MMP - SPECT

Micro SPECT: Measurement of a mouse bone skeleton with  $^{99m}\text{Tc-HDP}$

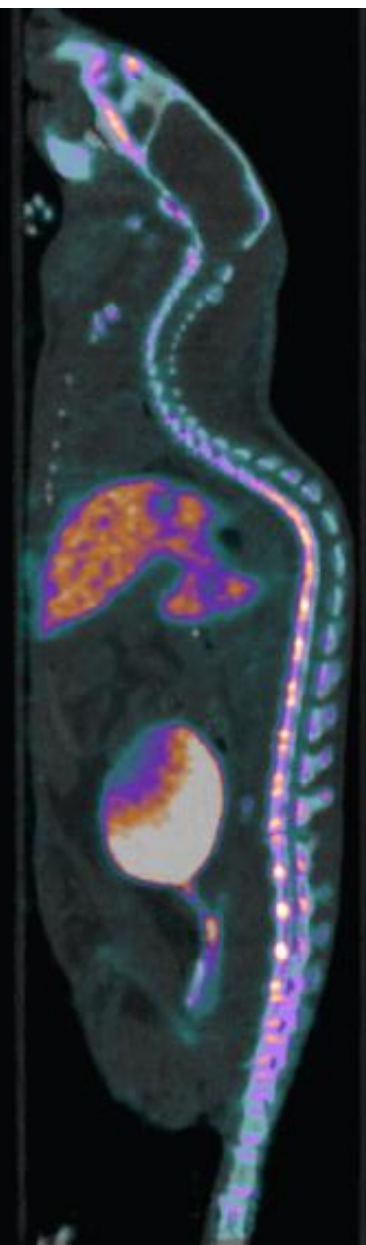
CT



$^{99m}\text{Tc-Hydroxy-Diphosphonat}$

Fusion

CT -  $^{99m}\text{Tc-HDP}$  SPECT





## Biodistribution of $^{123}\text{I}$ -5-iodo-4'-thio-2'-deoxyuridine ( $^{123}\text{I}$ -ITdU) in WiDr xenografted mouse models - MMP $\mu\text{SPECT}$ , 10.0 MBq 60 min p.i.

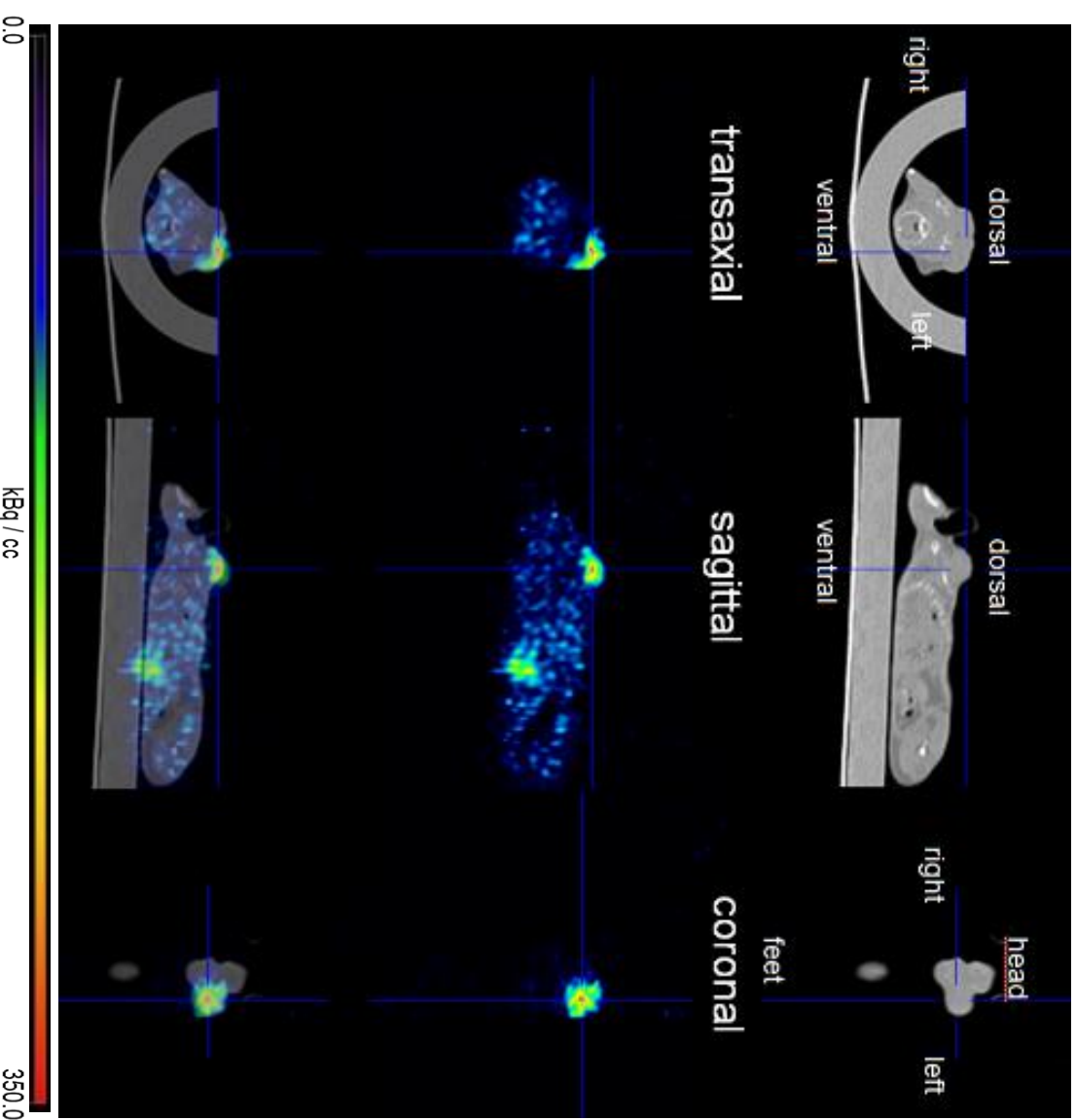
CT

$\mu\text{SPECT}$  [ $^{123}\text{I}$ ]-ITdU

FdUrd-Apppl.

Fusion

$\mu\text{SPECT}$  [ $^{123}\text{I}$ ]-ITdU  
+ CT



# Biodistribution of nucleosid analogues

PET [ $^{18}\text{F}$ ]FLT

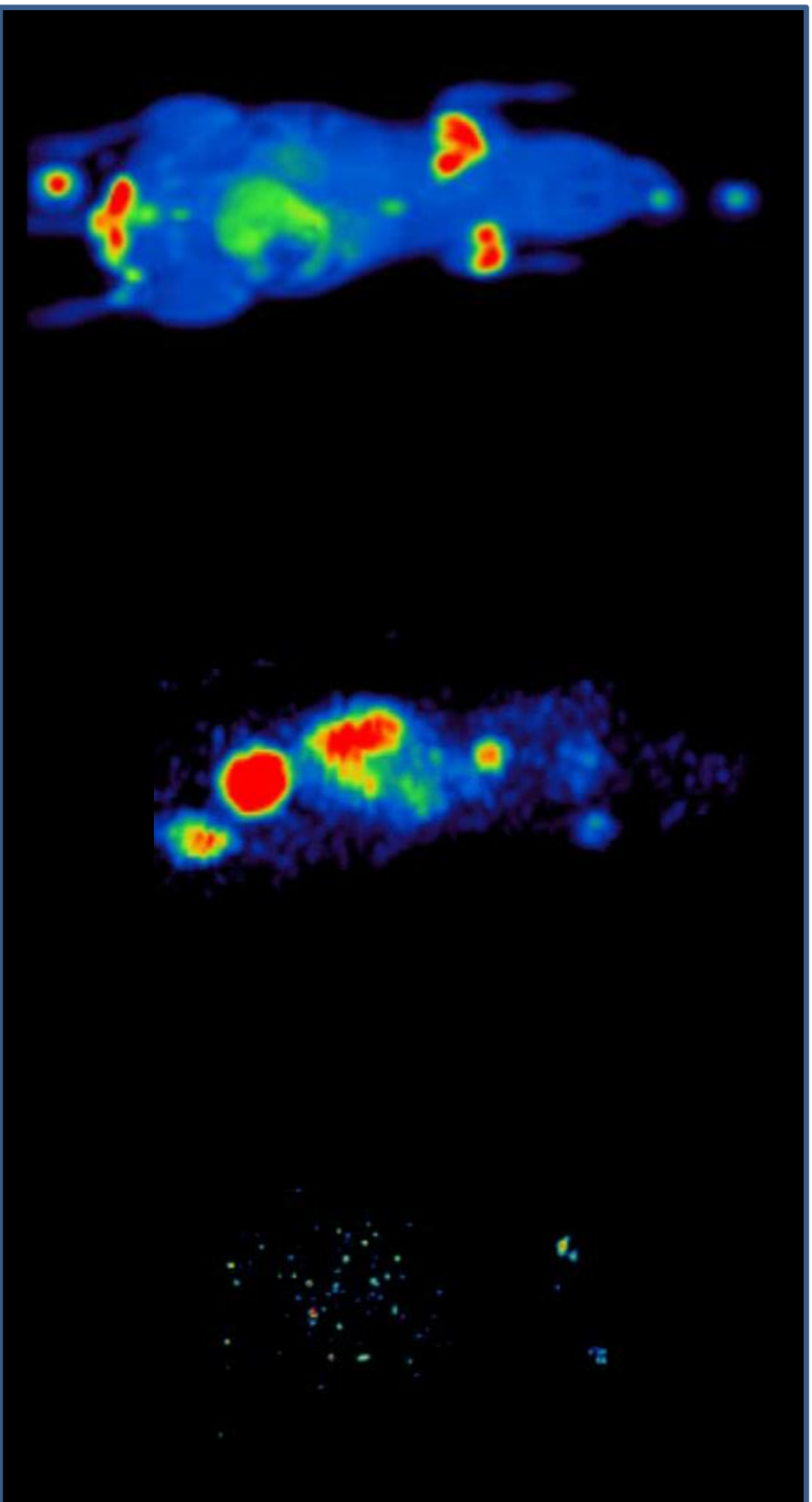
$\mu$ SPECT [ $^{123}\text{I}$ ]-ITdU

$\mu$ SPECT [ $^{123}\text{I}$ ]-ITdU

FdUrd-Appl.

FdUrd-Appl. 60 min p.i.

FdUrd-Appl. 24 h p.i.



0.0

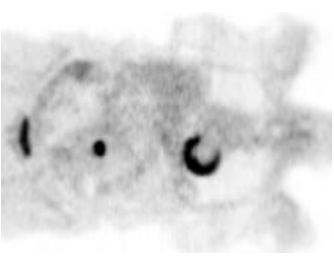
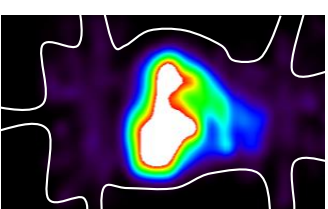
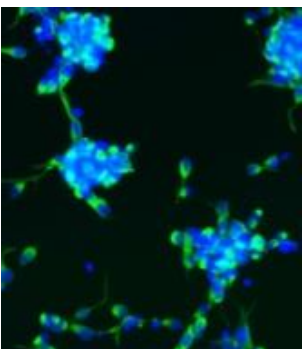
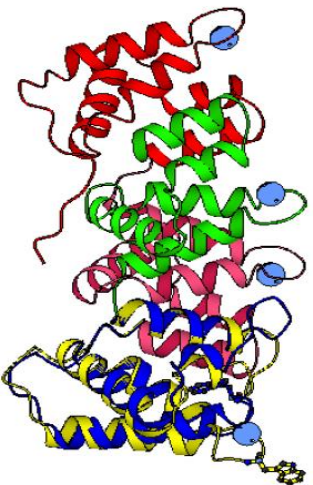
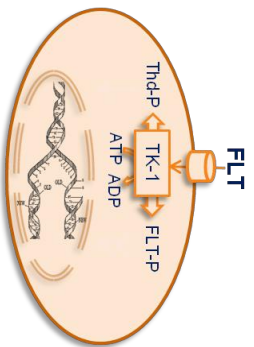
KBq / cc

830.0

# Examples for small animal imaging: biodistribution studies play a major role

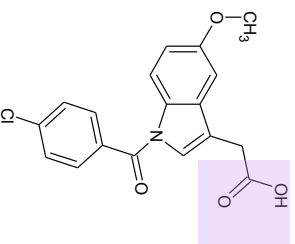
- New tracer development
- New pharmacokinetics development

- Therapeutic studies



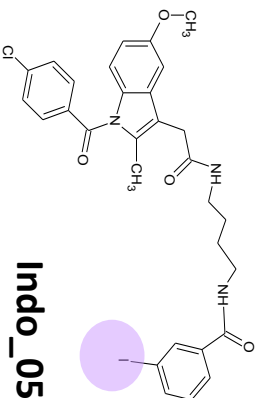
# Indomethacin derivatives targeting COX2

## Indomethacin as chemical lead

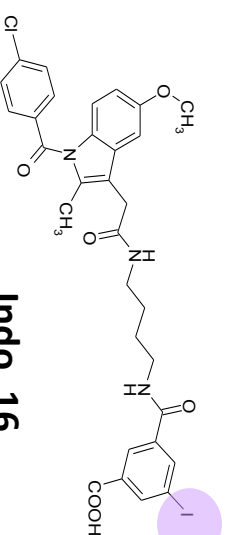


Derivatization at carboxylic acid  $\Rightarrow$  Indometacin-Derivate with different Polarity and

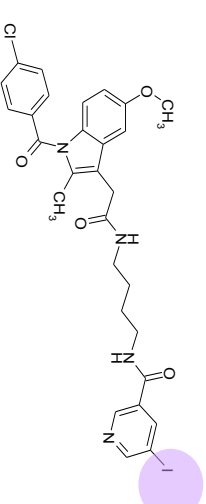
charge for labeling with radio iod und radio fluor



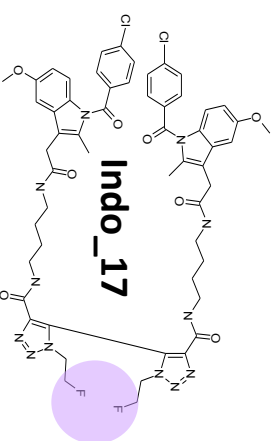
Indo\_05



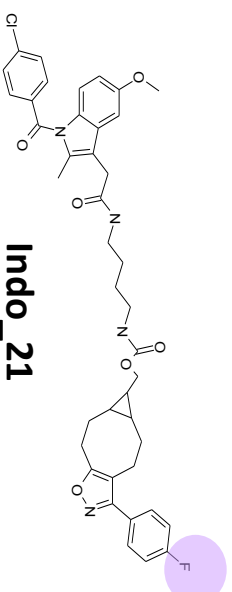
Indo\_16



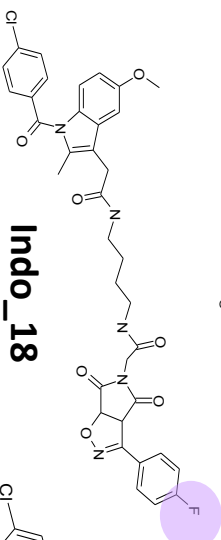
Indo\_23



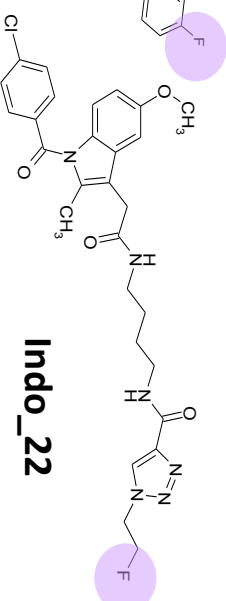
Indo\_17



Indo\_21



Indo\_18



Indo\_22

Cite this: Chem. Commun., 2012, 48, 7134–7136

www.rsc.org/chemcomm

### COMMUNICATION

Beyond azide–alkyne click reaction: easy access to  $^{18}\text{F}$ -labelled compounds *via* nitrile oxide cycloadditions†

Boris D. Zhitopolskiy,<sup>a,b</sup> René Kandler,<sup>c</sup> Diana Kohler,<sup>c</sup> Felix M. Mottaghy<sup>a,c</sup> and Bernd Nannacker<sup>a,b</sup>

Applied Radiation and Isotopes 71(2012) 184–192



C(4-[ $^{18}\text{F}$ ]fluorophenyl)-N-phenyl nitron: A novel  $^{18}\text{F}$ -labeled building block for metal free [ $3+2$ ]cycloaddition

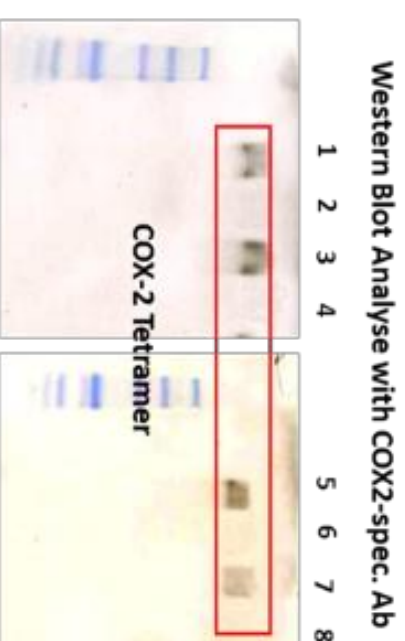
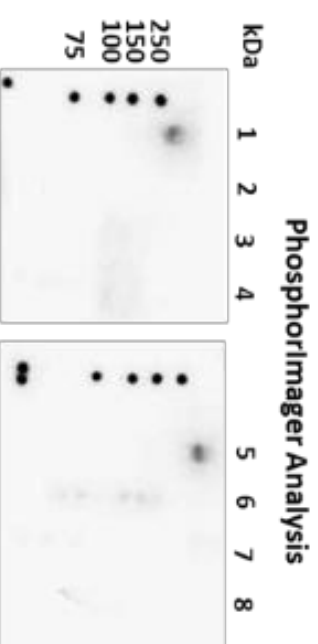
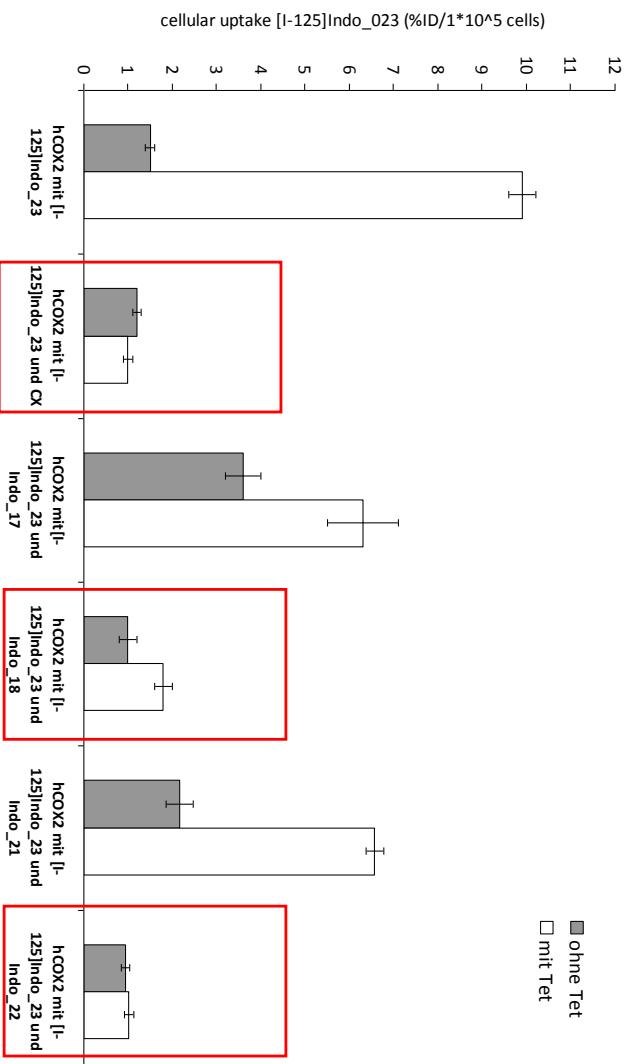
Boris D. Zhitopolskiy,<sup>a,b</sup> René Kandler,<sup>c</sup> Felix M. Mottaghy<sup>b,c</sup>, Bernd Nannacker<sup>a,c</sup>

<sup>a</sup> Institut für Radiochemie, Medizinische Fakultät, Universität zu Köln, 50931 Köln, Germany  
<sup>b</sup> Institut für Radiochemie, Medizinische Fakultät, Universität zu Köln, 50931 Köln, Germany  
<sup>c</sup> Department of Nuclear Medicine, Maastricht University Medical Center, P. Debylaan 25, 6201 RB Maastricht, the Netherlands



# COX2-specific Inhibitors: PET-Tracer

Cellular uptake of COX2-PET Tracer: Competition  
study with cold standards and  
[l-125]Indo\_23 as COX2 Tracer und corresponding  
Phosphorimager and Western Blot Analysis



1. HEK COX-2 mit [l-125]Indo\_23, Tet stimulated
2. HEK COX-2 [l-125]Indo\_23, unstimulated
3. HEK COX-2 mit [l-125]Indo\_23 + CX, Tet stimulated
4. HEK COX-2 mit [l-125]Indo\_23 + CX, unstimulated
5. HEK COX-2 mit [l-125]Indo\_23 + Indo\_21, Tet stimulated
6. HEK COX-2 mit [l-125]Indo\_23 + Indo\_21 unstimulated
7. HEK COX-2 mit [l-125]Indo\_23 + Indo\_22, Tet stimulated
8. HEK COX-2 mit [l-125]Indo\_23 + Indo\_22, unstimulated

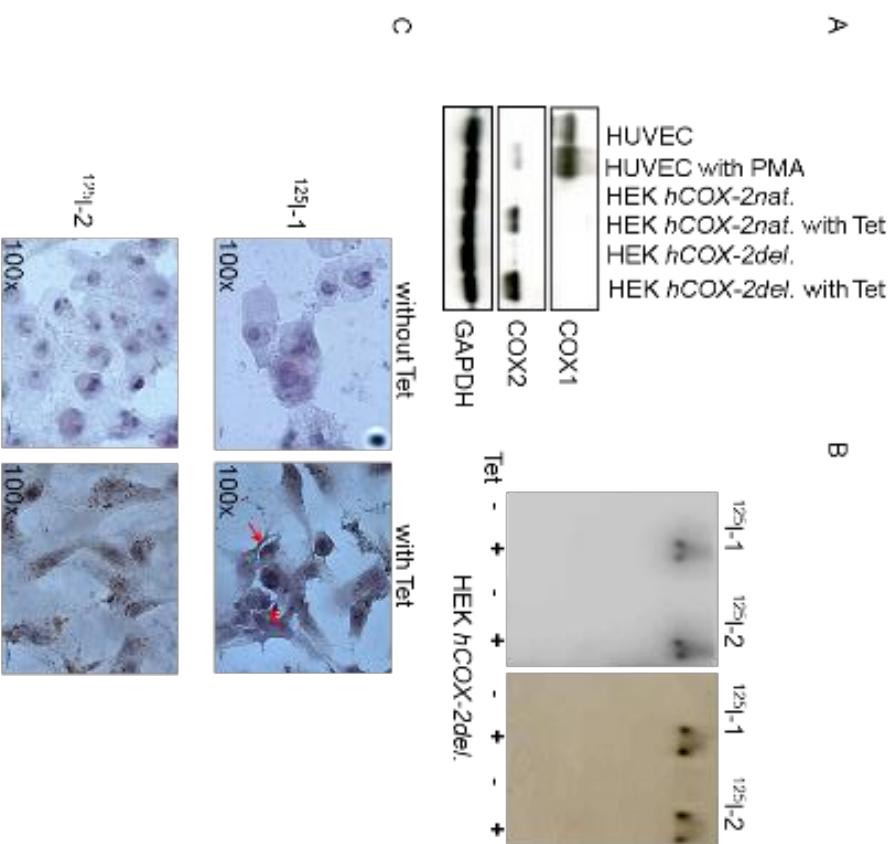


**Fig. 3.** Binding specificity and intracellular distribution of iodinated indomethacin derivatives. (A) SDS and western blot analysis of COX-1 and COX-2 expression in HUVEC, HEK *hCOX-2nat* and HEK *hCOX-2del* cells in dependency on PMA- and Tet-stimulation, respectively. GAPDH served as a loading control. (B) SDS gel electrophoresis of cell lysates obtained from HEK *hCOX-2del* cells incubated with  $^{125}\text{I}$ -1 and  $^{125}\text{I}$ -2 and visualized by phosphorimager (*left*); subsequent western blot analysis with COX-2 specific antibody. (C) Intracellular localization of  $^{125}\text{I}$ -1 and  $^{125}\text{I}$ -2 in HEK *hCOX-2del* cells detected by microautoradiography followed by a standard H&E staining.

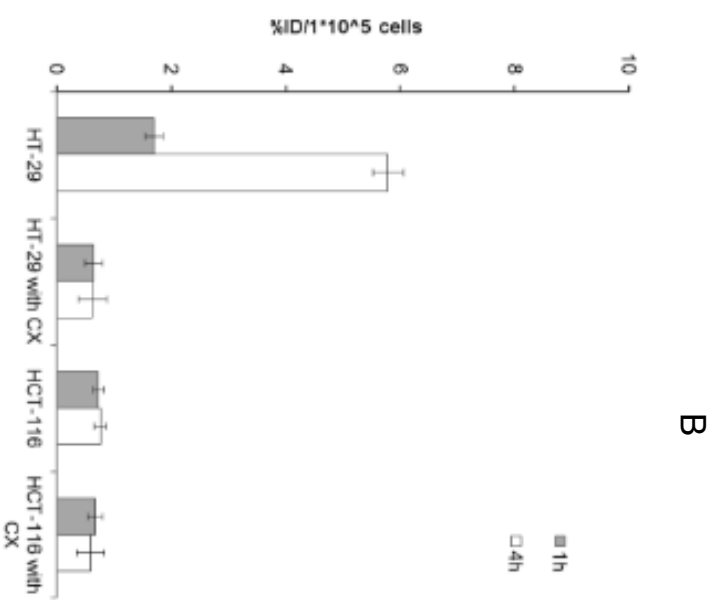
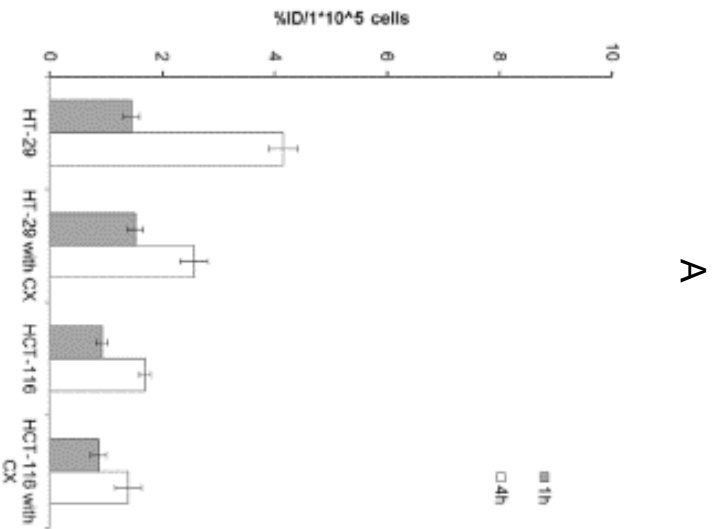


**Fig. 4.** Cellular uptake with  $^{125}\text{I}$ -1 and  $^{125}\text{I}$ -2 compounds in colon carcinoma cells after 1h and 4h incubation (in % of incubated dose (ID)/well). (A) Cellular uptake of  $^{125}\text{I}$ -1 in HT29 and HCT-116 cells w/o and with CX. (B) Cellular uptake of  $^{125}\text{I}$ -2 in HT29 and HCT-116 cells w/o and with CX.

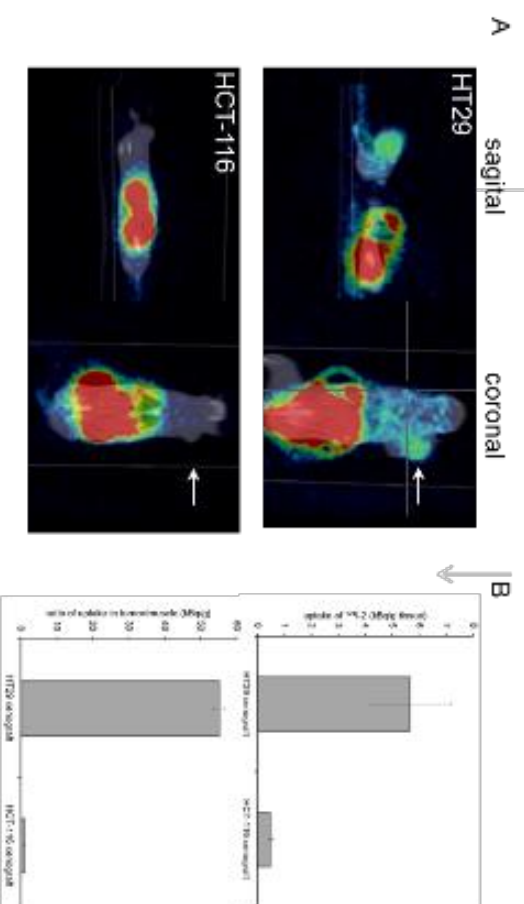
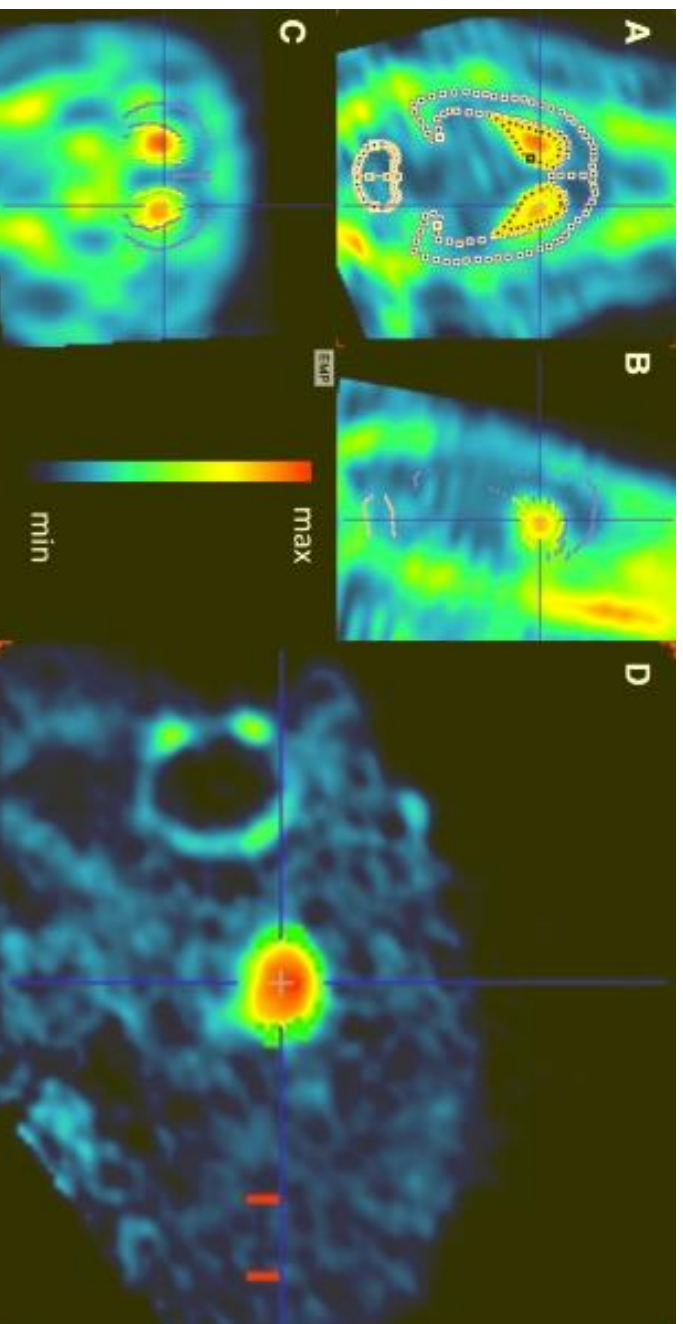
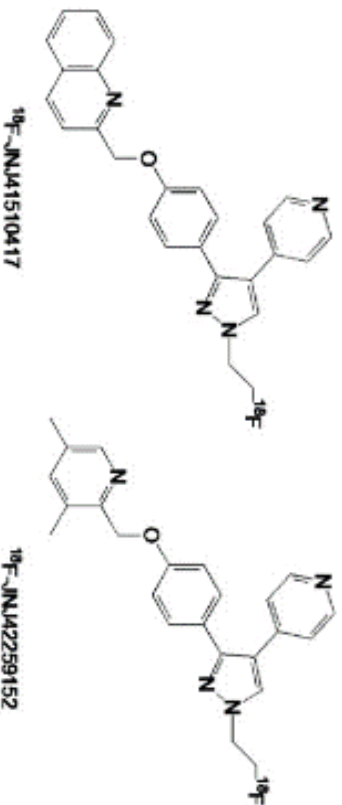


**Fig. 5.** *In vivo* study with  $^{124}\text{I}$ -**2** compound in colon carcinoma xenografted SCID mice. (A)  $\mu\text{PET}/\text{CT}$  molecular imaging of COX-2 with  $^{124}\text{I}$ -**1** in HT29 (upper panel) and HCT-116 (lower panel) xenografted SCID mice at 4h p.i.. (B) Uptake of  $^{125}\text{I}$ -**2** in HT29 and HCT-116 tumors (in KBq/g tissue) (upper panel); tumor to muscle uptake ratio of  $^{125}\text{I}$ -**2** in HT29 and HCT-116 tumor xenografted mice (lower panel). (C) immunohistological analysis of COX-1 and COX-2 in HT29 and HCT-116 xenografts.

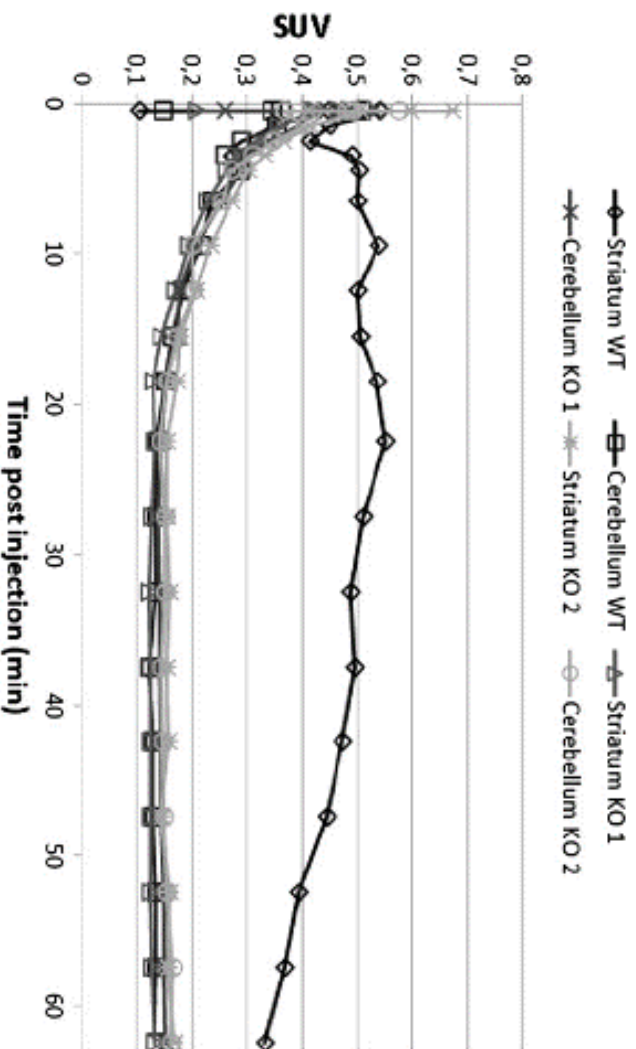


## New pharmaca development

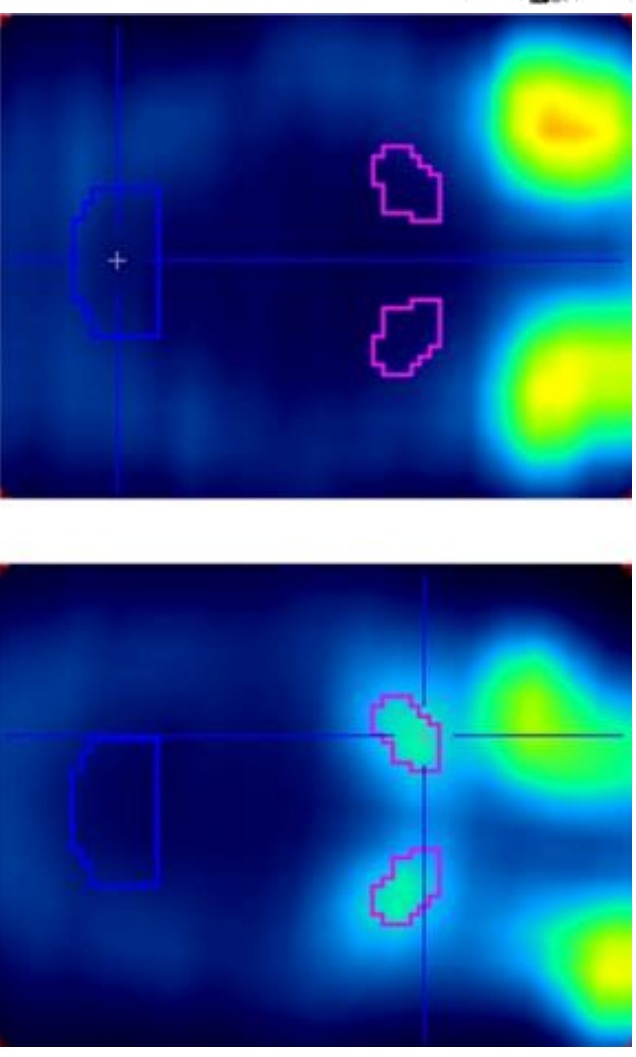
Phosphodiesterase-10A (PDE10A) is implicated in several neuropsychiatric disorders involving basal ganglia neurotransmission, such as schizophrenia, obsessive–compulsive disorder and Huntington's disease.



# New pharmaca development



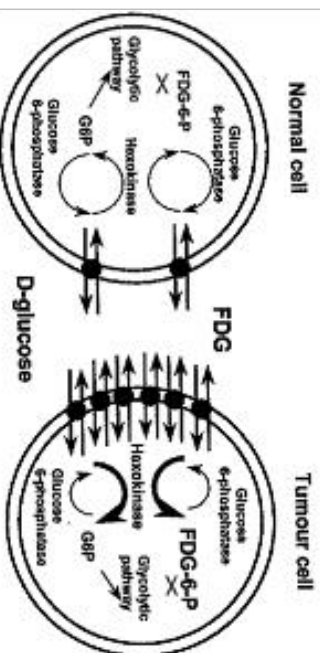
Small-animal PET transversal sections of KO (left image) and WT (right image) mouse brain injected with [18F]JNJ42259152 (summed images from 0 to 60 min post tracer injection). ROIs were drawn on the areas corresponding to striatum and cerebellum to obtain the TACs of [18F]JNJ42259152 in striatum and cerebellum of two PDE10A KO mice and one WT mouse (WT = wild type mouse, KO = PDE10A knock-out mouse).



S. Celen et al. *NeuroImage* 82:13–22, 2013

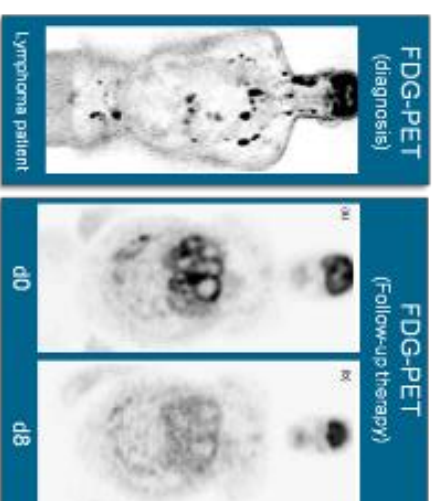
# Glucose metabolism: therapy response

## <sup>18</sup>F-FDG – PET



Eur J Nucl Med Mol Imaging (2010) 37:1688–1695  
DOI 10.1007/s00259-010-1479-0

ORIGINAL ARTICLE



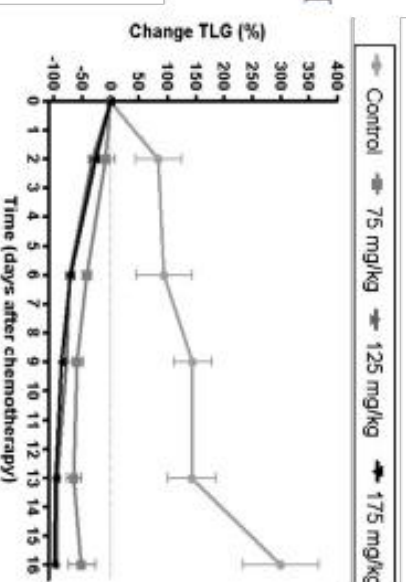
Stroobants et al., E J Cancer 2003

## Dose-response relationship in cyclophosphamide-treated B-cell lymphoma xenografts monitored with [<sup>18</sup>F]FDG PET

Liesbet Brepoels · Marijke De Sain-Hubert ·  
Siegfried Stroobants · Gregor Verhoef · Jan Balzarini ·  
Luc Morelmans · Felix M. Mottaghy

	Day 0	Day 2	Day 6	Day 9	Day 13	Day 16
Vol <sub>total</sub> (ml)	3.3	3.2	2.8	1.8	0.4	0.3
SAV <sub>total</sub> (ml/cm <sup>3</sup> )	8	9	2.9	4.4	2.1	3.3
SAV <sub>lymphoma</sub> (ml/cm <sup>3</sup> )	17.9	8.6	10.3	8.6	3.7	7.7
TLG <sub>lymphoma</sub>	28.5	16	8	7.2	0.9	1

→ [<sup>18</sup>F]FDG – Uptake represents dose-effect-dependency of Cyclophosphamid





# Proliferation: Therapy Response

## 18F-FLT – PET

Am J Nucl Med Mol Imaging 2012;2(1):110-121  
www.ajnmiml.us /ISSN:2160-8407/ajnmiml1111001

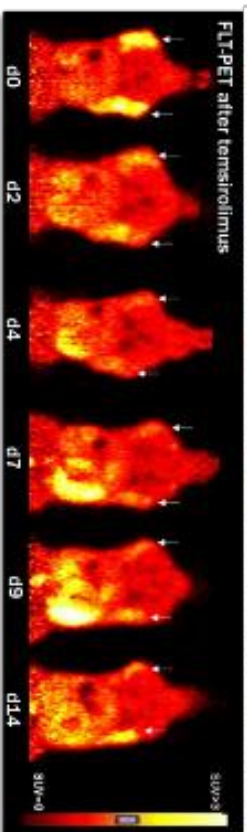
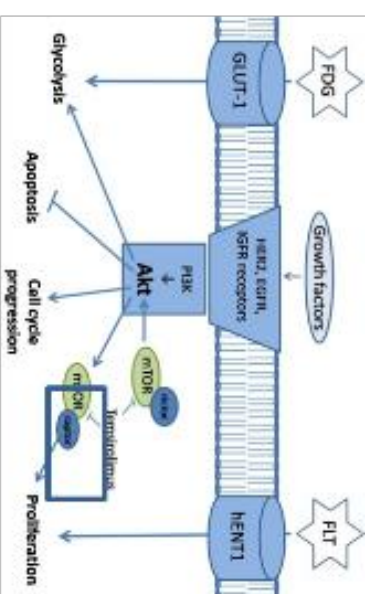
### Original Article

### Molecular imaging of therapy response with 18F-FLT and 18F-FDG following cyclophosphamide and mTOR inhibition

Manjike De Saint-Hubert<sup>1</sup>, Lieselot Brepoels<sup>2</sup>, Ellen Devos<sup>2</sup>, Peter Vermaelen<sup>2</sup>, Tjibe De Groot<sup>3</sup>, Thomas Tousseyn<sup>4</sup>, Luc Mortelmans<sup>2</sup>, Felix M Hottelaghy<sup>1,2,5</sup>

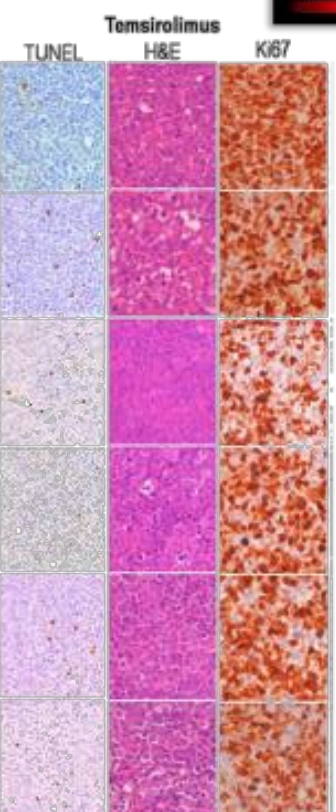
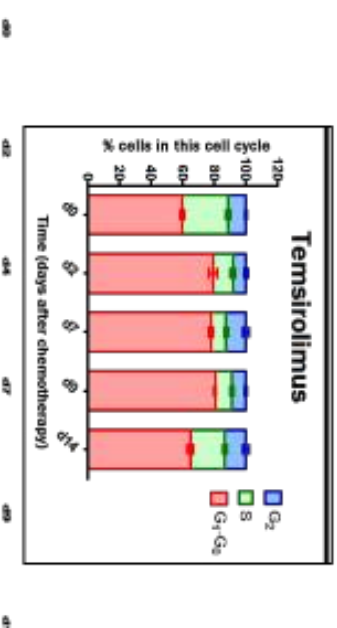
<sup>1</sup>Department of Nuclear Medicine, Maastricht University Medical Centre, Maastricht, The Netherlands; <sup>2</sup>Department of Nuclear Medicine, Katholieke Universiteit Leuven, Leuven, Belgium; <sup>3</sup>Laboratory for Radiopharmacy, Katholieke Universiteit Leuven, Leuven, Belgium; <sup>4</sup>Morphology and Molecular Pathology, Katholieke Universiteit Leuven, Leuven, Belgium; <sup>5</sup>Department of Nuclear Medicine, University Hospital RWTH Aachen, Germany

Received November 5, 2011; accepted November 18, 2011; Epub December 15, 2011; Published January 1, 2012



→ FLT-PET represents reduced proliferation after temsirolimus.

→ Correlates with the end of mitosis (Increase of G0/G1 in FACS) and ki67- staining





## Take home

- **SPECT and PET**
  - provide a broad spectrum of diagnostic approaches
  - help to understand biological processes
  - are an important link in the „bench to bedside“  
concept of probe development
- **Molecular Imaging**
  - is important for non-invasive monitoring of disease
  - supports development of new theranostic concepts